

AMPLITUDE BLOWUP IN COMPRESSIBLE EULER FLOWS WITHOUT SHOCK FORMATION

HELGE KRISTIAN JENSSEN

ABSTRACT. Recent works have demonstrated that continuous self-similar radial Euler flows can drive primary (non-differentiated) flow variables to infinity at the center of motion. Among the variables that blow up at collapse is the pressure, and it is unsurprising that this type of behavior can generate an outgoing shock wave.

In this work we prove that there is an alternative scenario in which an incoming, continuous 3-d flow suffers blowup, including in pressure, and yet remains continuous beyond collapse. We verify that this behavior is possible even in cases where the fluid is everywhere moving toward the center of motion at time of collapse. The results underscore the subtlety of shock formation in multi-dimensional flow.

Key words. Compressible fluid flow, multi-d Euler system, similarity solutions, radial symmetry, unbounded solutions

AMS subject classifications. 35L45, 35L67, 76N10, 35Q31

CONTENTS

1. Introduction	2
1.1. Main result and outline	3
2. Similarity variables and similarity ODEs	5
2.1. Similarity ODEs and reduced similarity ODE	6
2.2. Strategy and preliminary observations	6
3. Critical points of the reduced similarity ODE	8
3.1. Critical points on the V -axis	8
3.2. Critical points off the V -axis	9
3.3. P_6 - P_9 in isentropic case	10
3.4. Critical points at infinity	11
4. Restricting λ and κ in terms of n and γ	11
5. Presence, location, and types of P_4 - P_9	14
5.1. Preliminaries	14
5.2. Presence and locations of P_4 - P_9	16
5.3. Nodality of P_8, P_9	17
6. Further properties of critical points	19
6.1. Primary and secondary slopes at P_9	19
6.2. The node-saddle connection $P_9P_{-\infty}$	21
6.3. The critical points P_4 and P_5	22
7. Blowup solutions continuous away from the point of collapse	22
7.1. Analysis of the Σ trajectory	24
7.2. Proof of part (iv) of Theorem 1.1	26
8. Additional remarks	27
8.1. Blowup with a converging or diverging velocity field	27

Date: January 17, 2025.

1. INTRODUCTION

The non-isentropic Euler system describes the time evolution of a compressible fluid in the absence of viscosity and heat conduction:

$$\rho_t + \operatorname{div}_{\mathbf{x}}(\rho \mathbf{u}) = 0 \quad (1.1)$$

$$(\rho \mathbf{u})_t + \operatorname{div}_{\mathbf{x}}[\rho \mathbf{u} \otimes \mathbf{u}] + \operatorname{grad}_{\mathbf{x}} p = 0 \quad (1.2)$$

$$(\rho E)_t + \operatorname{div}_{\mathbf{x}}[(\rho E + p)\mathbf{u}] = 0. \quad (1.3)$$

The independent variables are time t and position $\mathbf{x} \in \mathbb{R}^n$ ($n = 2, 3$), and the dependent variables are density ρ , fluid velocity \mathbf{u} , and specific internal energy e ; the total energy density is $E = e + \frac{1}{2}|\mathbf{u}|^2$. We assume the fluid is an ideal gas with adiabatic index $\gamma > 1$, so that the pressure p is given by

$$p(\rho, e) = (\gamma - 1)\rho e, \quad (1.4)$$

and also polytropic, i.e., the specific internal energy is proportional to the absolute temperature θ of the gas. The sound speed c is then given by

$$c = \sqrt{\frac{\gamma p}{\rho}} = \sqrt{\gamma(\gamma - 1)e} \propto \sqrt{\theta}. \quad (1.5)$$

The unknowns ρ , \mathbf{u} , p , c , θ are referred to as primary (i.e., undifferentiated) flow variables.

In what follows we specialize to radial flows, i.e., solutions to (1.1)-(1.3) where the flow variables depend on position only through $r = |\mathbf{x}|$, and the velocity field is purely radial, i.e.,

$$\mathbf{u}(t, \mathbf{x}) = u(t, r) \frac{\mathbf{x}}{r}$$

Choosing ρ , u , c as dependent variables, the Euler system (1.1)-(1.3) reduces to

$$\rho_t + u\rho_r + \rho(u_r + \frac{(n-1)u}{r}) = 0 \quad (1.6)$$

$$u_t + uu_r + \frac{1}{\gamma\rho}(\rho c^2)_r = 0 \quad (1.7)$$

$$c_t + uc_r + \frac{\gamma-1}{2}c(u_r + \frac{(n-1)u}{r}) = 0 \quad (1.8)$$

where $r > 0$, $\rho = \rho(t, r)$, $u = u(t, r)$, and $c = c(t, r)$. In continuous Euler flow, the specific entropy S , specified via Gibbs' relation $de = \theta dS - pd(\frac{1}{\rho})$, is transported along particle paths. For continuous radial flows we therefore have

$$S_t + uS_r = 0. \quad (1.9)$$

Pioneering works by Guderley [5] and Landau-Stanyukovich [19] in the 1940s initiated the study of *self-similar* radial Euler flows. Self-similarity provides a radical simplification, reducing (1.6)-(1.8) to a system of three non-linear ODEs. A key observation is that the sub-system of ODEs for the similarity variables V and C corresponding to u and c , yields a single, autonomous ODE relating V and C (cf. (2.14) below). The upshot is that one can effectively analyze various types of self-similar Euler flows by studying a planar phase portrait. An important motivation for studying this type of solutions in detail is that they exhibit different types of singular behaviors. The present work concerns one aspect of this.

While the study of self-similar Euler solutions has generated a considerable literature by now (see, e.g. references in [9]), it is only lately that rigorous results have been obtained. Indeed, the existence of the converging-expanding shock flows originally studied by Guderley and Landau-Stanyukovich, has been established in a strict mathematical sense only very recently [8].

Another scenario, describing the collapse of a spherical cavity, was analyzed by Hunter [7]; see also [1]. Building on earlier works, Lazarus [14] provided a detailed, and partly numerical, analysis of the Guderley and Hunter solutions.

A different type of focusing solutions - the setting of the present work - is provided by *continuous* flows in which a converging wave collapses and blows up at the center of motion. One motivation for considering this latter type of solutions is to clarify the blowup mechanism. Specifically, that blowup is a pure focusing effect that can occur even in the presence of an everywhere positive pressure field (in contrast to the flows considered by Guderley, Landau-Stanyukovich, and Hunter.) A first, rigorous construction of continuous blowup was done in [11] for the simplified isothermal model: A continuous (but not C^1) wave converges toward the origin, collapses (implodes), and reflects off an expanding shock wave. A similar construction in [12] (depending on numerically drawn phase portraits) indicated the same type of behavior for the isentropic model.

A far more challenging task was accomplished in [15] where *smooth* (C^∞) self-similar blowup solutions were constructed (up to collapse) for the first time; see also [2]. In turn, these were used to generate nearby blowup solutions of the compressible Navier-Stokes system in [16] - a fundamental result in fluid dynamics. Recently, [3] shows how non-radial perturbations of the smooth imploding Euler profiles from [15] provide examples of vorticity blowup in compressible flow.

In a different direction, the work [9] considered self-similar Euler flows exhibiting another type of blowup behavior. These solutions remain locally bounded near the center of motion while several of the flow variables suffer gradient blowup at time of collapse. Somewhat surprisingly, [9] provides numerical evidence that such a scenario does not necessarily lead to shock formation in the ensuing flow, at least for sufficiently large values of the adiabatic index ($\gamma \gtrsim 10$). The main objective of the present work is to prove that this phenomenon, i.e., absence of shock formation, can occur even in the more singular case of amplitude blowup (for any $\gamma > 1$).

The challenging general problem of analyzing multi-d shock formation and propagation has been treated in a number of recent works, cf. Section 1.3.1. in [3] for a review. The present work illustrates one subtlety of shock formation, or rather lack thereof, by focusing (pun intended) attention on non-generic, converging-diverging symmetric flows.

1.1. Main result and outline. It is well-known that the radial Euler system (1.6)-(1.7)-(1.8) admits self-similar solutions, see [4, 5, 14, 17–19]. We follow the setup in [4, 14] and posit

$$x = \frac{t}{r^\lambda}, \quad \rho(t, r) = r^\kappa R(x), \quad u(t, r) = -\frac{r^{1-\lambda}}{\lambda} \frac{V(x)}{x}, \quad c(t, r) = -\frac{r^{1-\lambda}}{\lambda} \frac{C(x)}{x}, \quad (1.10)$$

where the similarity parameters κ and λ are a priori free. Our main findings are as follows:

Theorem 1.1. *Consider the 3-dimensional compressible Euler system (1.1)-(1.3) for an ideal gas (1.4) with adiabatic index $\gamma > 1$, and let the similarity parameter κ have the “isentropic” value $\bar{\kappa} = -\frac{2(\lambda-1)}{\gamma-1}$.*

Then, for any $\lambda > 1$ sufficiently close to 1 (depending on γ), the Euler system (1.1)-(1.3) admits radially symmetric, self-similar solutions of the form (1.10) with the following properties:

- (i) *They are defined on all of $\mathbb{R}_t \times \mathbb{R}_x^3$ and continuous except at the single point $(t, \mathbf{x}) = (0, 0)$;*
- (ii) *At time $t = 0$ the density, velocity, pressure, sound speed, and temperature all tend to infinity as the origin $\mathbf{x} = 0$ is approached;*
- (iii) *The solutions contain locally finite amounts of mass, momentum, and energy at all times, and describe globally isentropic, shock-free flows;*
- (iv) *There are solutions with the properties (i)-(iii) where in addition the fluid is everywhere flowing toward the center of motion at time $t = 0$. Similarly, there are other solutions satisfying (i)-(iii) in which the fluid is everywhere flowing away from the center at time $t = 0$.*

The rest of the paper is organized as follows. Section 2 provides the setup and records the similarity ODEs. These involve the space dimension n and the adiabatic constant γ , as well as two the similarity parameters κ and λ . (Throughout we mostly follow the notation in [14].) We also impose three constraints (C1)-(C3). The first requires locally finite amounts of the conserved quantities (cf. (iii) above); (C2) prescribes that blowup should occur at a single point in space-time (chosen as the origin); and (C3) concerns the types of the relevant critical points in the plane of self-similar variables. We also record some standard observations about the similarity ODEs and their critical points, as well as the existence of a (well-known) exact integral. Finally, it is recorded that (C1)-(C3) implies a particular value of one of the similarity parameters ($\kappa = \bar{\kappa}$), and it is verified that this in turn implies that the flow is globally isentropic.

Section 3 records the critical points of the similarity ODEs and analyzes their presence in the case of isentropic flow. The implications of constraints (C1)-(C3) are analyzed in Sections 4 and 5. Section 4 argues for the aforementioned “isentropic” value of $\kappa = \bar{\kappa}$ (this argument was also presented in [9, 13]), and Proposition 4.2 summarizes the relevant implications of this choice.

Section 5 deals with the arguments for how the second similarity parameter λ must be further restricted in terms of n and γ in order to satisfy constraint (C3). This takes the form of a series of increasingly restrictive upper bounds on λ . Although we do not evaluate analytically all of these constraints, we show that they are all met whenever $\lambda > 1$ is sufficiently close to 1 (for n and γ fixed). This will suffice for our needs. Section 6 provides further properties of the critical points; see Proposition 6.3 for a summary. Up to this point, most of the analysis is standard.

The main result, i.e. existence of radial self-similar Euler flows that suffer amplitude blowup at a single space-time point without generating a shock wave, is proved in Section 7. This is accomplished by exploiting one particular trajectory of the similarity ODEs, viz. the one that passes *vertically* through the origin in the (V, C) -plane. An argument based on barriers demonstrates that for $n = 3$ and any $\gamma > 1$, this trajectory joins the two nodal points P_8 and P_9 via the origin P_1 , whenever $\lambda > 1$ is sufficiently close to 1. In turn, P_8 and P_9 are connected by trajectories to two critical points at infinity ($P_{+\infty}$ and $P_{-\infty}$, respectively). Joining the various trajectories, we obtain a global solution of the similarity ODEs, and this yields the sought-for globally defined, shock-free 3-d Euler flow as described in Theorem 1.1.

The analysis will show that the particular trajectory under consideration approaches the nodes P_8 and P_9 along their primary direction. As a consequence there are nearby trajectories that, while still connecting P_8 to P_9 , pass *non-vertically* through the origin. These “perturbed” trajectories will have either positive or negative slopes at the origin in the (V, C) -plane. As a consequence, there are 3-d Euler flows which suffer amplitude blowup at $(t, r) = (0, 0)$, while remaining continuous everywhere else, and with the fluid at time $t = 0$ everywhere moving either toward or away from the center of motion (cf., part (iv) of Theorem 1.1).

The fact that blowup (including of density) can occur also when all particles are moving away from the origin might seem counterintuitive. It is perhaps more surprising that a shock is not necessarily generated even when the pressure blows up at the center of motion and all fluid particles move toward the origin at time of collapse. These issues are briefly discussed in Section 8.1.

Finally, in Section 8.2, we consider the issue of non-uniqueness (our original motivation). Namely, with blowup solutions of the type discussed above, one is really pushing the Euler system to (or beyond) its limits as a physical model. It is reasonable to ask if such solutions could be used to give examples of non-uniqueness. With solutions as described by Theorem 1.1, where in particular the pressure field becomes unbounded at a point, it would be reasonable to expect that an expanding shock should form. So, could it be that, upon freezing time at $t = 0$, the data of the constructed blowup solutions in Theorem 1.1 also admit a propagation for $t > 0$ which is discontinuous, and thus distinct from the solution described in Theorem 1.1? Section 8.2 outlines an analysis, based on

the Rankine-Hugoniot relations, which indicates (but does not conclusively prove) that the answer is negative.

Remark 1.1. *Concerning vacuum formation (vanishing of the density field) we have that:*

- *The solutions described in Theorem 1.1 do not exhibit vacuum formation; in particular, the density remains strictly positive at the center of motion for all times. On the other hand, vacuum is approached asymptotically as $r \rightarrow \infty$ at all times, and also along the center of motion as $t \rightarrow \pm\infty$; see Remarks 3.1 and 3.3.*
- *This is in contrast to Guderley shock solutions, i.e., radial, self-similar Euler flows in which an incoming shock propagates into a quiescent fluid near $r = 0$ for $t < 0$, [5, 14]. For such solutions, a one-point vacuum is present at the center of motion $r = 0$ for all times following collapse; see [10] (observation (O2), Section IV.C) and also the numerical plots in [14] (Figures 8.27–8.28). A one-point vacuum also occurs at and after collapse in the solutions considered in [9].*

2. SIMILARITY VARIABLES AND SIMILARITY ODES

The overall goal is to demonstrate existence of solutions to (1.6)-(1.7)-(1.8), with certain properties, for all times $t \in (-\infty, \infty)$ and all $r > 0$. This will be accomplished by building suitable solutions to the system of similarity ODEs (2.5)-(2.6) obtained by substituting the ansatz (1.10) into (1.6)-(1.7)-(1.8). As we seek globally defined Euler flows, we need to build solutions of the similarity ODEs (2.5)-(2.6) that are defined for all $x \in (-\infty, \infty)$.

We shall impose several constraints on the solutions of interest to us, and this will severely restrict the possible values that κ and λ can take. These constraints are:

- (C1) The total amounts of mass, momentum, and energy in any fixed ball about the origin in physical space should remain finite at all times.
- (C2) The solutions are to suffer amplitude blowup at the center of motion at time of collapse $t = 0$, and at no other place or time. In particular, $\rho(t, r)$, $u(t, r)$, $c(t, r)$ (and hence also $\theta(t, r)$ and $p(t, r)$, cf. (1.4)-(1.5)) should remain bounded as $r \downarrow 0$ whenever $t \neq 0$.
- (C3) Two of the critical points of the similarity ODEs (2.5)-(2.6) (points P_8 and P_9 in what follows) should be present as nodes, while its two critical points at infinity ($P_{\pm\infty}$) should be saddles that are approached as $|x| \rightarrow \infty$.

The precise implications of (C1)-(C3) will be detailed in later sections. For now we note that (C1) is a minimal requirement for physicality, while (C2) is imposed to focus attention on highly singular solutions that suffer amplitude blowup of primary flow variables. All solutions we consider will be such that both $\frac{V(x)}{x}$ and $\frac{C(x)}{x}$ tend to finite limits as $x \rightarrow 0$. By sending $t \rightarrow 0$ with $r > 0$ fixed in (1.10), we will therefore have

$$u(0, r), c(0, r) \propto r^{1-\lambda}. \tag{2.1}$$

In particular, as (C2) requires blowup of $u(0, r)$, $c(0, r)$ as $r \downarrow 0$, we shall only consider $\lambda > 1$. On the other hand, we shall exploit the fact that blowup occurs whenever $\lambda > 1$: our main result on continuous blowup will be established for λ sufficiently close to 1 (depending on γ).

Constraint (C3) is imposed in order to argue that there are unique trajectories of the reduced similarity ODE ((2.14) below) connecting the critical points P_8 and P_9 to its critical points $P_{\pm\infty}$ at infinity. It will also guarantee, for $\lambda \gtrsim 1$, that there are infinitely many trajectories of the similarity ODEs connecting P_8 and P_9 via the origin in the (V, C) -plane.

We note that for Guderley solutions, the similarity parameter κ must necessarily vanish (see p. 318 in [14]). In contrast, for the continuous flows considered in this work, (C1)-(C3) will imply that κ must take a non-zero value which is given in terms of λ and γ (cf. 2.20). This turns out to

imply that the flows we construct are in fact isentropic: the specific entropy is globally constant in space and time, cf. Section 4.

Remark 2.1. *Theorem 1.1 is formulated for 3-dimensional flows with spherical symmetry. However, most of the analysis applies also to the case of cylindrical symmetry $n = 2$. As will be clear from what follows, it is only one part of the final barrier argument in Section 7.1.1 that requires $n = 3$. It would be of interest to know if the extra dimension is really required for the blowup behavior described in Theorem 1.1.*

2.1. Similarity ODEs and reduced similarity ODE. The self-similar ansatz (1.10) reduces (1.6)-(1.7)-(1.8) to a system of three *similarity ODEs* for $R(x)$, $V(x)$, $C(x)$. A calculation shows that these are given by ($' \equiv \frac{d}{dx}$)

$$(1 + V)R' + RV' = \frac{\kappa+n}{\lambda x} RV \quad (2.2)$$

$$C^2 R' + \gamma R(1 + V)V' + 2RCC' = \frac{1}{\lambda x} [\gamma(\lambda + V)V + (\kappa + 2)C^2]R \quad (2.3)$$

$$\frac{\gamma-1}{2} CV' + (1 + V)C' = \frac{1}{\lambda x} [\lambda + (1 + \frac{n(\gamma-1)}{2})V]C, \quad (2.4)$$

where we observe that (2.4) does not involve R . An essential observation, due Guderley [5], is that R can be eliminated from (2.3) by using (2.2). We thus obtain two ODEs for only V and C . Solving these for V' and C' yields

$$V' = -\frac{1}{\lambda x} \frac{G(V,C)}{D(V,C)} \quad (2.5)$$

$$C' = -\frac{1}{\lambda x} \frac{F(V,C)}{D(V,C)}, \quad (2.6)$$

with

$$D(V, C) = (1 + V)^2 - C^2 \quad (2.7)$$

$$G(V, C) = nC^2(V - V_*) - V(1 + V)(\lambda + V) \quad (2.8)$$

$$F(V, C) = C[C^2(1 + \frac{\alpha}{1+V}) - k_1(1 + V)^2 + k_2(1 + V) - k_3], \quad (2.9)$$

where

$$V_* = \frac{\kappa-2(\lambda-1)}{n\gamma}, \quad (2.10)$$

$$\alpha = \frac{1}{\gamma}[(\lambda - 1) + \frac{\kappa}{2}(\gamma - 1)], \quad (2.11)$$

and

$$k_1 = 1 + \frac{(n-1)(\gamma-1)}{2}, \quad k_2 = \frac{(n-1)(\gamma-1) + (\gamma-3)(\lambda-1)}{2}, \quad k_3 = \frac{(\gamma-1)(\lambda-1)}{2}. \quad (2.12)$$

We note that

$$k_1 - k_2 + k_3 = \lambda. \quad (2.13)$$

Finally, (2.5)-(2.6) give the single *reduced similarity ODE*

$$\frac{dC}{dV} = \frac{F(V, C)}{G(V, C)} \quad (2.14)$$

which relates V and C along self-similar Euler flows.

2.2. Strategy and preliminary observations. We start by noting that, although the phase plane analysis of (2.14) is central to the analysis, what is really required for building Euler flows of the form (1.10), are suitable solutions of (2.5)-(2.6). And the latter system is not equivalent to the single ODE (2.14): In contrast to (2.14), the system (2.5)-(2.6) degenerates along the *critical (sonic) lines*

$$L_{\pm} := \{C = \pm(1 + V)\}, \quad (2.15)$$

across which the numerator D in (2.5)-(2.6) changes sign. A direct calculation verifies that

$$F(V, \pm(1+V)) \equiv \mp \frac{(\gamma-1)}{2} G(V, \pm(1+V)), \quad (2.16)$$

i.e., F and G are proportional along L_{\pm} . Therefore, if a trajectory Γ of the reduced similarity ODE (2.14) crosses one of the critical lines L_{\pm} at a point P where one (and hence both) of F and G is non-zero, then the flow of (2.5)-(2.6) along Γ is directed in opposite directions on either side of the critical line at P . The upshot is that such a trajectory Γ cannot be used to generate a physically meaningful Euler flow.

This implies a drastic reduction of the set of relevant trajectories: Any continuous crossing of one of the critical lines L_{\pm} by a trajectory of (2.14) must occur at a ‘‘triple point’’ where $F = G = D = 0$. As we shall see, the existence of triple points off the V -axis amounts to the statement that the aforementioned critical points P_8 and P_9 are present.

2.2.1. Strategy and an exact integral. We can now be somewhat more precise about the general strategy for building continuous radial self-similar Euler flows. Assuming we have identified a suitable solution $C(V)$ of the reduced similarity ODE (2.14) (in particular, crossing L_{\pm} at triple points), we solve (2.5) with $C = C(V)$ to obtain $V = \hat{V}(x)$. Assuming further that this yields a global solution (i.e., $\hat{V}(x)$ is defined for all $x \in (-\infty, \infty)$), we obtain a globally defined $\hat{C}(x) := C(\hat{V}(x))$. In turn, $\hat{V}(x)$ and $\hat{C}(x)$ define, via (1.10), the flow variables $u(t, r)$ and $c(t, r)$ in an Euler flow.

To determine the density field $\rho(t, r)$, we may solve (2.2) (with $V = \hat{V}(x)$) for $R = \hat{R}(x)$. However, the similarity ODEs (2.2)-(2.4) admit an exact ‘‘adiabatic’’ integral (see Eqn. (2.7) in [14], or pp. 319-320 in [17]). This may be deduced as follows. For an ideal polytropic gas, the specific entropy S is a function of $\rho^{1-\gamma}\theta \propto \rho^{1-\gamma}c^2$. For a self-similar flow (1.10) it follows that

$$S = \text{function of } r^{-2\gamma\alpha}\sigma(x) \quad \text{where} \quad \sigma(x) := R(x)^{1-\gamma}\left(\frac{C(x)}{x}\right)^2, \quad (2.17)$$

and α is given by (2.11). Equation (1.9) therefore becomes

$$(1+V)\sigma' + 2\gamma\alpha\frac{V}{\lambda x}\sigma = 0.$$

Multiplying through by R , and substituting for $\frac{RV}{\lambda x}$ from the right-hand side of (2.2), results in

$$R(1+V)\sigma' + \frac{2\gamma\alpha}{\kappa+n}[R(1+V)]'\sigma = 0.$$

It follows that

$$[R|1+V|^q R(x)^{1-\gamma}\left(\frac{C(x)}{x}\right)^2] \equiv \text{const.} > 0, \quad (2.18)$$

where

$$q = \frac{2\gamma\alpha}{\kappa+n} \equiv \frac{1}{\kappa+n}[\kappa(\gamma-1) + 2(\lambda-1)]. \quad (2.19)$$

For later use, we record the following special case: When κ takes the value

$$\bar{\kappa} = \bar{\kappa}(\gamma, \lambda) := -\frac{2(\lambda-1)}{\gamma-1}, \quad (2.20)$$

the constants α and q vanish, and (2.18) reduces to

$$\left(\frac{C(x)}{x}\right)^2 R(x)^{1-\gamma} \equiv \text{const.} > 0. \quad (2.21)$$

According to (2.17), this means that the specific entropy S in this case takes a constant value throughout any continuous part of the flow. Thus, when we construct a globally continuous self-similar Euler flow (1.10) with $\kappa = \bar{\kappa}$, we necessarily obtain an isentropic flow (i.e., S takes on a constant value globally in space-time). We therefore refer to $\bar{\kappa}$ as the *isentropic* κ -value. We shall see in Section 4 that this value is in fact a consequence of the constraints (C1)-(C3) above.

2.2.2. *Preliminaries about critical points.* To build our self-similar flows we need to analyze the critical points of (2.14) in some detail. These are the common zeros of the functions F and G , and their number and locations depend on $n, \gamma, \lambda, \kappa$. It turns out that some of these are necessarily located on the critical lines (cf. (2.15)); they thus provide triple points where trajectories of (2.14) can cross L_{\pm} .

The zero-levels of F and G are denoted

$$\mathcal{F} = \{(V, C) \mid F(V, C) = 0\} \quad \mathcal{G} = \{(V, C) \mid G(V, C) = 0\},$$

and we note that $V = V_*$ (cf. (2.10)) is a vertical asymptote for \mathcal{G} . Finally, we record the symmetries

$$G(V, -C) = G(V, C) \quad \text{and} \quad F(V, -C) = -F(V, C). \quad (2.22)$$

In particular, trajectories of (2.14) in the (V, C) -plane are located symmetrically about the V -axis, and critical points off the V -axis come in symmetric pairs.

3. CRITICAL POINTS OF THE REDUCED SIMILARITY ODE

A complete recording of the critical points of (2.14), for all values of $(n, \gamma, \lambda, \kappa)$, was recently given in [9], and we shall only review the relevant findings. We assume $n = 2$ ($m = 1$) or $n = 3$ ($m = 2$) and $\gamma > 1$. Until further notice, λ and κ are considered as free parameters.

There are up to nine critical points of (2.14), and these come in two groups (notation as in [9, 14]): P_1 - P_3 located along the V -axis, and three pairs P_4 - P_5 , P_6 - P_7 , and P_8 - P_9 , with each pair of points located off and, according to (2.22), symmetrically about the V -axis. There are two further critical points at infinity, viz.

$$P_{\pm\infty} := (V_*, \pm\infty). \quad (3.1)$$

The points $P_{\pm\infty}$, analyzed in Section 3.4 below, are central to the construction of continuous Euler flows: These are the states that the relevant solutions $(V(x), C(x))$ of (2.5)-(2.6) tend to as $x \rightarrow \mp\infty$, respectively.

3.1. Critical points on the V -axis. From (2.8)-(2.9) we have $F(V, 0) \equiv 0$ and $G(V, 0) = V(1 + V)(\lambda + V)$. Therefore, there are in general three critical points located on the V -axis, viz.

$$P_1 = (0, 0) \quad P_2 = (-1, 0) \quad P_3 = (-\lambda, 0),$$

of which only P_1 is relevant in the present work. The linearization of (2.14) at P_1 is $\frac{dC}{dV} = \frac{C}{V}$. Thus, P_1 is a star point: Whenever \mathcal{L} is a straight half-line from P_1 , there is a unique trajectory $(V, C(V))$ of (2.14) that approaches P_1 tangent to \mathcal{L} (cf. Theorem 3.6, pp. 218-219 in [6]).

We need to analyze how the corresponding solutions $(V(x), C(x))$ of the system (2.5)-(2.6) behave as P_1 is approached. Assume \mathcal{L} has slope ℓ , so that $C(V) \approx \ell V$ for $V \approx 0$ along the solution in question. Substitution into (2.5)-(2.6), and use of (2.13), show that

$$\frac{dV}{dx} \approx \frac{V}{x} \quad \text{and} \quad \frac{dC}{dx} \approx \frac{C}{x} \quad \text{as } P_1 \text{ is approached.}$$

It follows that any solution to (2.5)-(2.6) which approaches P_1 must do so as $x \rightarrow 0$. Furthermore, the limits

$$\nu = \lim_{x \rightarrow 0} \frac{V(x)}{x} \quad \text{and} \quad \omega = \lim_{x \rightarrow 0} \frac{C(x)}{x} \quad \text{exist as finite numbers, and } \ell = \frac{\omega}{\nu}. \quad (3.2)$$

With these notations we can specify precisely the velocity and sound speed at time of collapse in the corresponding Euler flow (cf. (2.1)). Sending $t \rightarrow 0$ with $r > 0$ fixed, (1.10) and (3.2) give

$$u(0, r) = -\frac{\nu}{\lambda} r^{1-\lambda} \quad \text{and} \quad c(0, r) = -\frac{\omega}{\lambda} r^{1-\lambda}. \quad (3.3)$$

We note that $\omega = 0$ gives $\ell = 0$, which corresponds to the two flat trajectories $C(V) \equiv 0$, for $V \geq 0$, of (2.14). Also, the limiting case $\nu = 0$ gives $\ell = \pm\infty$, which corresponds to the two trajectories of (2.14) that reach P_1 vertically. The latter trajectories will be of particular interest to us.

Remark 3.1. *The behavior of $C(x)$ as $x \rightarrow 0$ yields information about the asymptotic behavior of the sound speed and density in the far field as $r \rightarrow \infty$. In particular, with $\kappa = \bar{\kappa}$ (isentropic flow) we obtain from (1.10)₄ and (3.2)₂ that*

$$\rho(t, r) \propto c(t, r)^{\frac{2}{\gamma-1}} \sim \left(\frac{|\omega|}{\lambda}\right)^{\frac{2}{\gamma-1}} r^{\bar{\kappa}} \quad \text{as } r \rightarrow \infty. \quad (3.4)$$

Since $\bar{\kappa} < 0$ for $\lambda > 1$, this shows that the density decays to zero in the far field for the solutions described in Theorem 1.1.

We next analyze how solutions to (2.5)-(2.6) pass through P_1 . Recall that the sound speed c is non-negative by definition (cf. (1.5)), and that we only consider positive λ -values (in fact, $\lambda > 1$). It therefore follows from (1.10)₄ that a solution $(V(x), C(x))$ of (2.5)-(2.6) which passes through the origin must do so by moving from the upper half-plane $\{C > 0\}$ to the lower half-plane $\{C < 0\}$ as x increases from negative to positive values. In particular, this shows that $\omega \leq 0$. In fact, since $\omega = 0$ corresponds to the flat trajectories $C(V) \equiv 0$ ($V \geq 0$), we have $\omega < 0$ for any trajectory considered in the following.

On the other hand, the sign of ν depends on whether the origin P_1 is approached from within the 1st or 2nd quadrant in the (V, C) -plane. For later reference we note that, according to (3.3)₁, the sign of ν determines the direction of the flow at time of collapse $t = 0$:

- Case 1: If $\ell = \frac{\omega}{\nu} > 0$, i.e., the solution approaches P_1 from within the 1st quadrant, then $\nu < 0$ and $u(0, r) > 0$ for all $r > 0$. Thus $\ell > 0$ corresponds to an everywhere diverging flow at time of collapse.
- Case 2: If $\ell = \frac{\omega}{\nu} < 0$, i.e., the solution approaches P_1 from within the 2nd quadrant, then $\nu > 0$ and $u(0, r) < 0$ for all $r > 0$. Thus $\ell < 0$ corresponds to an everywhere converging flow at time of collapse.

These observations will be relevant for part (iv) of Theorem 1.1; see Section 7.2.

Remark 3.2. *As we shall see below, the solutions $(V(x), C(x))$ we construct connect the critical point P_8 to the origin P_1 . Since P_8 will be located in the 2nd quadrant (see Proposition 6.3), we obtain that if Case 1 occurs, then the solution trajectory must cross the C -axis on its way from P_8 to P_1 . Thus, $V(x)$ must vanish for some $x = \bar{x} < 0$, which means that the corresponding flow exhibits stagnation, i.e., vanishing velocity, along the path $\bar{r}(t) = (\frac{t}{\bar{x}})^{\frac{1}{\lambda}}$ prior to collapse ($t < 0$).*

Similarly, in Case 2, the flows we consider will necessarily exhibit stagnation after collapse.

The issue of blowup with a diverging or converging flow at time of collapse is addressed further in Section 8.1.

3.2. Critical points off the V -axis. The critical points $P_i = (V_i, C_i)$, $i = 4, \dots, 9$, are identified by first solving for C^2 in terms of V from $G(V, C) = 0$, i.e.,

$$C^2 = g(V) := \frac{V(1+V)(\lambda+V)}{n(V-V_*)}, \quad (3.5)$$

and then using the result in $F(V, C) = 0$. This gives a cubic equation for V which has one real root $V_4 = V_5$ for any choice of $n, \gamma, \lambda, \kappa$. The remaining V -quadratic has real roots $V_6 = V_7$ and $V_8 = V_9$ only in certain cases, and these give the critical points P_6 - P_9 (when present).

Referring to [9] for details, we only record the results. For labeling we follow Lazarus [14] and let P_4, P_6, P_8 be the critical points located in the upper half-plane $\{C > 0\}$, while the points P_5, P_7, P_9 , respectively, are located symmetrically about the V -axis in the lower half-plane.

The points $P_4 = (V_4, C_4)$ and $P_5 = (V_4, -C_4)$ are given by

$$V_4 = -\frac{2\lambda}{2+n(\gamma-1)}, \quad C_4 = \sqrt{g(V_4)}. \quad (3.6)$$

Note that $g(V_4)$ may be negative, in which case P_4 and P_5 are not present. However, we shall see that they are necessarily present whenever the constraints (C1)-(C3) are met (see Lemma 5.3).

It is convenient to set

$$V_6 = V_7 \equiv V_- \quad \text{and} \quad V_8 = V_9 \equiv V_+.$$

A calculation shows that these are given by

$$V_{\pm} = \frac{1}{2m\gamma} \left[(\gamma - 2)\mu + \kappa - m\gamma \pm \sqrt{(\gamma - 2)^2\mu^2 - 2[\gamma m(\gamma + 2) - \kappa(\gamma - 2)]\mu + (\gamma m + \kappa)^2} \right], \quad (3.7)$$

where $m = n - 1$, and $\mu = \lambda - 1$.

Notation 1. *To shorten some of the expressions in what follows, we will freely use either n or m , λ or μ , and γ or ε , always assuming*

$$m = n - 1, \quad \mu = \lambda - 1, \quad \varepsilon = \gamma - 1.$$

Note that our standing assumptions imply $m \geq 1$, $\mu > 0$, and $\varepsilon > 0$.

It follows from (3.5) and (3.7) that the critical points P_6 - P_9 are present if and only if, first, the radicand in (3.7) is positive, and second, $g(V_{\pm}) > 0$. If so, we get the critical points

$$P_6 = (V_-, C_-), \quad P_7 = (V_-, -C_-), \quad P_8 = (V_+, C_+), \quad \text{and} \quad P_9 = (V_+, -C_+), \quad (3.8)$$

where

$$C_{\pm} = \sqrt{g(V_{\pm})}.$$

Note that P_6 (P_7) coalesces with P_8 (P_9 , respectively) whenever $V_+ = V_-$. This occurs for certain values of the parameters n , γ , λ ; see (A)-(B) below.

A direct calculation reveals that

$$C_{\pm}^2 = (1 + V_{\pm})^2, \quad (3.9)$$

so that P_6 - P_9 , when present, are located along the critical lines L_{\pm} .

3.3. P_6 - P_9 in isentropic case. We proceed to analyze the presence of P_6 - P_9 in the special case when κ takes the isentropic value $\bar{\kappa}$ in (2.20) (as will be seen to be dictated by the constraints (C1)-(C3)):

$$\bar{\kappa} = -\frac{2(\lambda-1)}{\gamma-1} \equiv -\frac{2\mu}{\varepsilon}.$$

In this case (3.7) gives

$$V_{\pm} = \frac{1}{2}(\mathbf{a}_n \pm \sqrt{\mathfrak{Q}_n}), \quad (3.10)$$

where

$$\mathbf{a}_n = \mathbf{a}_n(\gamma, \lambda) = \frac{(\varepsilon-2)}{m\varepsilon}\mu - 1 \quad \text{and} \quad \mathfrak{Q}_n = \mathfrak{Q}_n(\gamma, \lambda) = \left(\frac{\varepsilon-2}{m\varepsilon}\right)^2\mu^2 - 2\frac{(\varepsilon+2)}{m\varepsilon}\mu + 1. \quad (3.11)$$

A necessary condition for P_6 - P_9 to be present is that $\mathfrak{Q}_n \geq 0$ in (3.10), and there are two cases:

- (A) If $\gamma \neq 3$, then \mathfrak{Q}_n is quadratic in μ , and a calculation shows that $\mathfrak{Q}_n \geq 0$ if and only if $\lambda \leq \hat{\lambda}_n(\gamma)$ or $\lambda \geq \check{\lambda}_n(\gamma)$, where

$$\hat{\lambda}_n(\gamma) := 1 + \frac{(n-1)(\gamma-1)}{(\gamma+1)+\sqrt{8(\gamma-1)}} \quad (3.12)$$

and

$$\check{\lambda}_n(\gamma) = 1 + \frac{(n-1)(\gamma-1)}{(\gamma+1)-\sqrt{8(\gamma-1)}}. \quad (3.13)$$

In this case, $V_+ = V_-$ if and only if either $\lambda = \hat{\lambda}_n(\gamma)$ or $\lambda = \check{\lambda}_n(\gamma)$.

- (B) If $\gamma = 3$, then \mathfrak{Q}_n is linear in μ , and a calculation shows that $\mathfrak{Q}_n \geq 0$ if and only if $\lambda \leq \hat{\lambda}_n(3) \equiv 1 + \frac{n-1}{4}$. Also, $V_+ = V_-$ if and only if $\lambda = \hat{\lambda}_n(3)$.

We shall later provide sufficient conditions for the presence of P_6 - P_9 ; see Section 5.2.

3.4. Critical points at infinity. The critical points at infinity for (2.14), viz. $P_{\pm\infty} = (V_*, \pm\infty)$, will serve as end states at $x = \mp\infty$, respectively, of the sought-for solutions $(V(x), C(x))$ to (2.5)-(2.6). According to constraint (C3), we shall want there to be a unique $P_9P_{-\infty}$ -trajectory of (2.14). (From (2.22) it follows that there is then a unique $P_{+\infty}P_8$ -trajectory as well, viz. the reflection of the $P_9P_{-\infty}$ -trajectory about the V -axis.) At the same time, we want there to be infinitely many P_8P_9 -trajectories that pass through $P_1 = (0, 0)$. We therefore require that P_8 and P_9 are nodes and that $P_{\pm\infty}$ are saddles for (2.14) (cf. constraint (C3)).

The critical points at infinity are most easily analyzed by switching to the variables $w := V - V_*$ and $z := C^{-2}$ (thus treating $P_{\pm\infty}$ simultaneously). Linearizing the resulting equation for $\frac{dz}{dw}$ about $(w, z) = (0, 0)$ yields

$$\frac{dz}{dw} = \frac{Az}{Bz - nw}, \quad (3.14)$$

with

$$A = 2\left(1 + \frac{\alpha}{1+V_*}\right), \quad B = V_*(1 + V_*)(\lambda + V_*). \quad (3.15)$$

It follows that $P_{\pm\infty}$ are saddle points if and only if $A > 0$. This is clearly satisfied when $\kappa = \bar{\kappa}$ (since then $\alpha = 0$ and $A = 2$). For the remainder of this section $A > 0$ is assumed.

As indicated above, we need to argue that there is a unique $P_9P_{-\infty}$ -trajectory. We postpone this argument till Section 6.2 when the relative locations of \mathcal{F} , \mathcal{G} , and trajectories of (2.14) near P_9 have been determined. We therefore take the existence of the $P_9P_{-\infty}$ - and $P_{+\infty}P_8$ -solutions to (2.5)-(2.6) as given for now, and use (3.14) to obtain their behavior near $P_{\pm\infty}$.

The solutions $(w(x), z(x))$ of (3.14) correspond to solutions of (2.5)-(2.6) tending to $P_{\pm\infty}$ approach $(0, 0)$, and they do so tangent to the stable subspace of (3.14) at $(0, 0)$. According to (3.14), this subspace is $\{z = \frac{n+A}{B}w\}$, and it follows that $C(x)^2(V(x) - V_*) \sim \frac{B}{n+A}$ as $x \rightarrow \pm\infty$ for the solutions in question. Using this information in (2.5), and simplifying the expressions as $V(x) \rightarrow V_*$, shows that to leading order, $V'(x) \sim -\frac{A}{\lambda x}(V(x) - V_*)$. It follows that the solutions of (2.5)-(2.6) which approach the saddle points $P_{\pm\infty}$, do so to leading order as follows:

$$|V(x) - V_*| \sim |x|^{-\frac{A}{\lambda}} \quad \text{and} \quad C(x) \sim \mp|x|^{\frac{A}{2\lambda}} \quad \text{as } x \rightarrow \pm\infty. \quad (3.16)$$

Remark 3.3. *The asymptotic behavior of $C(x)$ as $|x| \rightarrow \infty$ yields information about the values of sound speed and density along the center of motion. In particular, with $\kappa = \bar{\kappa}$ (isentropic flow) we have $A = 2$, so that to leading order*

$$|C(x)| \sim x^{\frac{1}{\lambda}} \quad \text{as } x \rightarrow +\infty. \quad (3.17)$$

As $\rho \propto c^{\frac{2}{\gamma-1}}$ in isentropic flow, (3.17) therefore gives, for a fixed time $t > 0$, that

$$\rho(t, r) \propto c(t, r)^{\frac{2}{\gamma-1}} = \left(\frac{r^{1-\lambda}}{\lambda} \frac{|C(x)|}{x}\right)^{\frac{2}{\gamma-1}} \sim kt^{\frac{\bar{\kappa}}{\lambda}} \quad \text{as } r \downarrow 0,$$

where k is a strictly positive constant. This shows that no vacuum occurs along the center of motion at positive times in the solutions described by Theorem 1.1 (except asymptotically as $t \rightarrow \infty$). The same applies to negative times.

The only other way vacuum could occur would be by having $\lim_{x \rightarrow 0} \frac{C(x)}{x} \equiv \omega = 0$ (cf. (3.2)). However, as argued above in Section 3.1, $\omega < 0$ for solutions under consideration.

4. RESTRICTING λ AND κ IN TERMS OF n AND γ

In this section and the next we provide analytic formulations and consequences of the three constraints (C1)-(C3), and see how they delimit the possible values of the similarity parameters κ and λ . Recall the standing assumptions that $n = 2$ or 3 , $\gamma > 1$, and $\lambda > 1$.

Constraint (C1) requires that the integrals

$$\int_0^{\bar{r}} \rho(t, r) r^m dr, \quad \int_0^{\bar{r}} \rho(t, r) |u(t, r)| r^m dr, \quad \int_0^{\bar{r}} \rho(t, r) (e(t, r) + \frac{1}{2} |u(t, r)|^2) r^m dr \quad (4.1)$$

are finite at all times t and for all finite $\bar{r} > 0$. As we shall see below, the second part of constraint (C2) will imply that the solutions we construct are bounded near $r = 0$ at all times $t \neq 0$. For our present purposes it therefore suffices to impose (C1) at time of collapse $t = 0$. By using (3.3) together with $\rho(0, r) = R(0)r^\kappa$, we get that (4.1) holds at time $t = 0$ if and only if

- (I) $\kappa + n > 0$
- (II) $\lambda < 1 + \kappa + n$
- (III) $\lambda < 1 + \frac{\kappa + n}{2}$.

Clearly, (II) is a consequence of (I) and (III). For later use we note that (III) and $\gamma > 1$ give

$$0 < \frac{n + \kappa - 2(\lambda - 1)}{n\gamma} < \frac{n\gamma + \kappa - 2(\lambda - 1)}{n\gamma} \equiv 1 + V_*, \quad (4.2)$$

where V_* is given in (2.10).

We proceed to address the second part of constraint (C2). For this we assume, in accordance with constraint (C3), that we have selected a solution $(V(x), C(x))$ of (2.5)-(2.6) which approaches $P_{\pm\infty}$ as $x \rightarrow \mp\infty$. In the following argument we fix a time $t \neq 0$. We then have, by (1.10)₁, $|x| \propto r^{-\lambda}$ so that $r \downarrow 0$ corresponds to $|x| \rightarrow \infty$.

Now, (C2) requires that the primary flow variables ρ , u , c remain bounded as the center of motion $r = 0$ is approached. Consider first the speed

$$u(t, r) = -\frac{r^{1-\lambda}}{\lambda} \frac{V(x)}{x} = -\frac{r}{\lambda t} V(x) \propto V(x)r. \quad (4.3)$$

According to (3.16)₁ we have $V(x) \rightarrow V_*$ as $|x| \rightarrow \infty$, and it follows that $u(t, r) \sim r$ as $r \downarrow 0$. I.e., at any time different from the time of collapse $t = 0$, the speed of the fluid vanishes at a linear rate as the center of motion $r = 0$ is approached. Thus, boundedness (in fact, vanishing) of the fluid velocity as $r \downarrow 0$, does not imply any further constraints.

Next, consider the sound speed $c(t, r)$ as $r \downarrow 0$. From (3.16)₂ and $|x| \propto r^{-\lambda}$ we get

$$c(t, r) = -\frac{r}{\lambda t} C(x) \sim r^{1-\frac{A}{2}} \quad \text{as } r \downarrow 0. \quad (4.4)$$

Thus, boundedness of $c(t, r)$ as $r \downarrow 0$ requires $A \leq 2$. According to (3.15)₁ and (4.2), this amounts to

$$\alpha \leq 0. \quad (4.5)$$

Finally, consider the density field $\rho(t, r)$ as $r \downarrow 0$. Using (1.10)₂, the adiabatic integral (2.18), (4.2), and (3.16)₁, we have

$$\rho(t, r) = r^\kappa R(x) \sim r^\kappa \left(\frac{x}{C(x)}\right)^{\frac{2}{1-\gamma+q}},$$

where q is given in (2.19). Using again (3.16)₂ and $|x| \propto r^{-\lambda}$, we get

$$\rho(t, r) \sim r^{\kappa + \frac{A-2\lambda}{1-\gamma+q}} \quad \text{as } r \downarrow 0.$$

Thus, boundedness of $\rho(t, r)$ as $r \downarrow 0$ requires

$$\kappa + \frac{A-2\lambda}{1-\gamma+q} \geq 0. \quad (4.6)$$

We proceed to show that, under the integrability constraints (I)-(III), this last inequality together with (4.5) yield $\alpha = 0$. First, recall from (2.19) that $q = \frac{2\gamma\alpha}{\kappa+n}$; in particular, (4.5) and (I) give $q \leq 0$. As $\gamma > 1$ we therefore have $1 - \gamma + q < 0$, so that (4.6) may be rewritten as

$$\kappa(1 - \gamma + q) + A - 2\lambda \leq 0.$$

Substituting $q = \frac{2\gamma\alpha}{\kappa+n}$ and $A = 2(1 + \frac{\alpha}{1+V_*})$, and rearranging, we obtain the equivalent inequality

$$\left(\frac{\gamma\kappa}{\kappa+n} + \frac{1}{1+V_*}\right)\alpha \leq (\lambda - 1) + \frac{\kappa}{2}(\gamma - 1) \equiv \alpha\gamma, \quad (4.7)$$

cf. (2.11). Now assume for contradiction that $\alpha < 0$. According (2.11) we then have

$$\lambda < 1 - \frac{\kappa}{2}(\gamma - 1), \quad (4.8)$$

while (4.7) gives

$$\frac{1}{1+V_*} \geq \frac{\gamma n}{\kappa+n}. \quad (4.9)$$

According to (I) and (4.2), both $\kappa + n$ and $1 + V_*$ are strictly positive quantities. Using this in (4.9), and also the expression (2.10) for V_* , we rewrite (4.9) as

$$\lambda \geq 1 + \frac{n}{2}(\gamma - 1),$$

which together with (4.8) gives

$$1 + \frac{n}{2}(\gamma - 1) < 1 - \frac{\kappa}{2}(\gamma - 1) \quad \text{or} \quad (\kappa + n)(\gamma - 1) < 0.$$

As $\gamma > 1$ we obtain $\kappa + n < 0$, in contradiction to (I). Therefore, α cannot be strictly negative, and (4.5) gives $\alpha = 0$.

Opting to keep λ as a parameter, it follows from the expression (2.11) that the similarity parameter κ takes the isentropic value $\bar{\kappa}$ in (2.20). We have established the following:

Lemma 4.1. *Consider a radial, self-similar solution of the form (1.10) to the Euler system (1.6)-(1.7)-(1.8). Assume that the solution satisfies the constraints (C1)-(C3). Then the similarity parameter κ must necessarily take the value*

$$\bar{\kappa} = \bar{\kappa}(\gamma, \lambda) := -\frac{2(\lambda-1)}{\gamma-1}, \quad (4.10)$$

and the flow is therefore globally isentropic (cf. (2.21)).

Remark 4.1. *Conversely, it is evident from the calculations above that with $n = 2$ or $n = 3$, $\gamma > 1$, and $\lambda > 1$ given, the choice $\kappa = \bar{\kappa}(\gamma, \lambda)$ guarantees that the constraint (C2) is satisfied.*

Before proceeding we record some consequences of Lemma 4.1. First, observe that (4.10) is equivalent to $\alpha = 0$, so that (3.15) gives $A > 0$, which is the condition guaranteeing that $P_{\pm\infty}$ are saddles. In particular, the isentropic κ -value in (4.10) is consistent with the second part of constraint (C3).

Next, consider the inequalities (I)-(III). A calculation shows that, with $\kappa = \bar{\kappa}$, they reduce to the single constraint

$$\lambda < \tilde{\lambda}_n(\gamma) := 1 + \frac{n}{2}\left(1 - \frac{1}{\gamma}\right). \quad (4.11)$$

Also, as detailed in Section 3.1, amplitude blowup in $u(t, r)$ and $c(t, r)$ at time $t = 0$ requires $\lambda > 1$. It follows that $\bar{\kappa} < 0$; in particular, it follows from (1.10)₂ that also the density $\rho(t, r)$ suffers blowup at collapse. We note that (1.4)-(1.5) implies that the same applies to the temperature $\theta \propto c^2$ and pressure $p \propto \rho\theta$.

From here on the following assumptions are in force:

$$n = 2 \quad \text{or} \quad n = 3, \quad \gamma > 1, \quad \kappa = \bar{\kappa}(\gamma, \lambda), \quad 1 < \lambda < \tilde{\lambda}_n(\gamma). \quad (4.12)$$

Note that, with the isentropic κ -value, we have (cf. (2.10))

$$V_* = -\frac{2(\lambda-1)}{n(\gamma-1)} = -\frac{2\mu}{n\varepsilon} < 0. \quad (4.13)$$

Summing up the analysis above we have:

Proposition 4.2. *Assume (4.12) holds. Then the constraints (C1) and (C2), and also the second part of constraint (C3) concerning $P_{\pm\infty}$, are all met.*

As we shall see below, the λ -range in (4.12) will be delimited further by the requirement that the critical points P_8 and P_9 are present as nodes (i.e., the first part of constraint (C3)).

5. PRESENCE, LOCATION, AND TYPES OF P_4 - P_9

With the assumptions (4.12) in force, we proceed to analyze when the critical points P_8 and P_9 are present, and if so, when they are nodes.

5.1. Preliminaries. Necessary conditions for the presence of P_8 and P_9 were listed in (A)-(B) in Section 3.2. For $\gamma \neq 3$ they involve the two functions $\hat{\lambda}_n(\gamma)$ and $\tilde{\lambda}_n(\gamma)$, which satisfy $\hat{\lambda}_n(\gamma) < \tilde{\lambda}_n(\gamma)$ (cf. (3.12)-(3.13)). To avoid dealing with a number of sub-cases, we choose the lower λ -value and require

$$1 < \lambda < \hat{\lambda}_n(\gamma) = 1 + \frac{(n-1)(\gamma-1)}{(\gamma+1)+\sqrt{8(\gamma-1)}}, \quad (5.1)$$

for any n, γ under consideration (including $\gamma = 3$). Under this requirement we have $\mathfrak{Q}_n(\gamma, \lambda) > 0$ for all n, γ, λ under consideration. In particular, this implies that P_6, P_7, P_8, P_9 , when present, are four distinct points.

Before proceeding we compare the constraint (5.1) with the standing assumption in (4.11). It is immediate to verify that for $n = 2$, $\hat{\lambda}_2(\gamma) < \tilde{\lambda}_2(\gamma)$ for all $\gamma > 1$. On the other hand, for $n = 3$ and $\gamma > 1$, $\hat{\lambda}_3(\gamma) < \tilde{\lambda}_3(\gamma)$ holds if and only if $1 < \gamma < \gamma_+ := 3(13 + 4\sqrt{10}) \approx 76.9$. Defining

$$\lambda_2^*(\gamma) := \hat{\lambda}_2(\gamma) \quad (5.2)$$

and

$$\lambda_3^*(\gamma) := \begin{cases} \hat{\lambda}_3(\gamma) & \text{when } n = 3 \text{ and } 1 < \gamma < \gamma_+ \\ \tilde{\lambda}_3(\gamma) & \text{when } n = 3 \text{ and } \gamma \geq \gamma_+, \end{cases} \quad (5.3)$$

we therefore have the following:

Lemma 5.1. *For $n = 2$ or $n = 3$, $\gamma > 1$, and $\kappa = \bar{\kappa}(\gamma, \lambda)$, the conditions (C1) and (C2) are met and the radicand $\mathfrak{Q}_n(\gamma, \lambda)$ in (3.10) (determining V_{\pm}) is strictly positive whenever*

$$1 < \lambda < \lambda_n^*(\gamma). \quad (5.4)$$

We now assume (5.4) is met. The following analysis will show that, for n and γ fixed, the λ -range needs to be restricted further in order to meet the constraint (C3). For this we begin by deriving conditions for having the pair of points P_4, P_5 located to the left of the pair of points P_8, P_9 in the (V, C) -plane, i.e., we seek conditions guaranteeing that

$$V_4 < V_+, \quad (5.5)$$

cf. (3.6) and (3.8). The inequality (5.5) is relevant for two reasons: With n and γ fixed, and under suitable conditions on λ , it will be used to argue that P_4 - P_9 are all present, and that P_8, P_9 are nodes.

Substituting from (3.6) and (3.10)-(3.11) and rearranging show that (5.5) is equivalent to

$$\sqrt{\mathfrak{q}_n(\gamma, \lambda)} > A_n(\gamma, \lambda), \quad (5.6)$$

where

$$\mathfrak{q}_n(\gamma, \lambda) := m^2 \varepsilon^2 \mathfrak{Q}_n(\gamma, \lambda) = (\varepsilon - 2)^2 \mu^2 - 2m\varepsilon(\varepsilon + 2)\mu + m^2 \varepsilon^2, \quad (5.7)$$

and

$$A_n(\gamma, \lambda) := \frac{m\varepsilon}{2+\varepsilon} [n\varepsilon - 2(2\mu + 1)] - (\varepsilon - 2)\mu.$$

To analyze (5.6) it is convenient to consider the cases $n = 2$ and $n = 3$ separately. The calculations are elementary but somewhat lengthy, and we omit some of the details.

5.1.1. $V_4 < V_+$ for $n = 2$. With $n = 2$, (5.6) takes the form

$$\sqrt{\mathfrak{q}_2(\gamma, \lambda)} > A_2(\gamma, \lambda) \equiv \frac{(\gamma+1)}{\gamma}(2-\gamma)\left[\lambda - \frac{2\gamma}{\gamma+1}\right]. \quad (5.8)$$

A direct calculation using (5.1) and (5.3) verifies that $\lambda_2^*(\gamma) < \frac{2\gamma}{\gamma+1}$ for all $\gamma > 1$. Therefore, under the current assumption that $1 < \lambda < \lambda_2^*(\gamma)$, the square-bracketed term on the right-hand side of the inequality in (5.8) is negative. In particular, for $1 < \gamma \leq 2$, $A_2(\gamma, \lambda)$ is non-positive, and thus (5.6) holds, i.e., $V_4 < V_+$ in this case.

For $\gamma > 2$ the situation is more involved: $A_2(\gamma, \lambda)$ is then strictly positive for $1 < \lambda < \lambda_2^*(\gamma)$, and we need to evaluate the inequality in (5.8). Squaring both sides and rearranging we get that $V_4 < V_+$ now holds if and only if

$$(\gamma^2 - 2\gamma - 1)(\lambda - 1)^2 + 2(\gamma^2 - 1)(\lambda - 1) - (\gamma - 1)^2 < 0. \quad (5.9)$$

A calculation verifies that that (5.9) holds whenever $\gamma > 2$ and $1 < \lambda < \frac{\gamma\sqrt{2}}{\gamma+\sqrt{2}-1}$. A further calculation shows that the upper limit in the last expression satisfies $\frac{\gamma\sqrt{2}}{\gamma+\sqrt{2}-1} < \lambda_2^*(\gamma)$ for all $\gamma > 2$. We therefore delimit the λ -range further by setting

$$\lambda_2^\circ(\gamma) := \begin{cases} \hat{\lambda}_2(\gamma) = 1 + \frac{\gamma-1}{(\gamma+1)+\sqrt{8(\gamma-1)}} & 1 < \gamma \leq 2 \\ \frac{\gamma\sqrt{2}}{\gamma+\sqrt{2}-1} & \gamma > 2, \end{cases} \quad (5.10)$$

and we require from now on that

$$1 < \lambda < \lambda_2^\circ(\gamma) \quad (5.11)$$

when $n = 2$ and $\gamma > 1$.

5.1.2. $V_4 < V_+$ for $n = 3$. The analysis is similar to the case $n = 2$. First, with $n = 3$, (5.6) takes the form

$$\sqrt{\mathfrak{q}_3(\gamma, \lambda)} > A_3(\gamma, \lambda) \equiv \frac{\gamma+1}{3\gamma-1}(5-3\gamma)\left[\lambda - \frac{3\gamma-1}{\gamma+1}\right]. \quad (5.12)$$

A direct calculation using (5.1) and (5.3) verifies that $\lambda_3^*(\gamma) < \frac{3\gamma-1}{\gamma+1}$ for all $\gamma > 1$. Therefore, under the current assumption that $1 < \lambda < \lambda_3^*(\gamma)$, the square-bracketed term on the right-hand side of the inequality in (5.12) is negative. In particular, for $1 < \gamma \leq \frac{5}{3}$, $A_3(\gamma, \lambda)$ is non-positive, and thus (5.6) holds, i.e., $V_4 < V_+$ in this case.

If instead $\gamma > \frac{5}{3}$, then $A_3(\gamma, \lambda)$ is strictly positive for $1 < \lambda < \lambda_3^*(\gamma)$, and we need to evaluate the inequality in (5.12). Squaring both sides and rearranging we get that $V_4 < V_+$ now holds if and only if

$$(3\gamma^2 - 6\gamma - 1)(\lambda - 1)^2 + 6(\gamma^2 - 1)(\lambda - 1) - 6(\gamma - 1)^2 < 0. \quad (5.13)$$

A calculation verifies that that (5.13) holds whenever $\gamma > \frac{5}{3}$ and $1 < \lambda < \frac{3\gamma-1}{\sqrt{3}(\gamma-1)+2}$. A further calculation shows that the upper limit in the last expression satisfies $\frac{3\gamma-1}{\sqrt{3}(\gamma-1)+2} < \lambda_3^*(\gamma)$ for all $\gamma > \frac{5}{3}$. We therefore delimit the λ -range further by setting

$$\lambda_3^\circ(\gamma) := \begin{cases} \lambda_3^*(\gamma) = 1 + \frac{2(\gamma-1)}{(\gamma+1)+\sqrt{8(\gamma-1)}} & 1 < \gamma \leq \frac{5}{3} \\ \frac{3\gamma-1}{\sqrt{3}(\gamma-1)+2} & \gamma > \frac{5}{3}, \end{cases} \quad (5.14)$$

and we require from now on that

$$1 < \lambda < \lambda_3^\circ(\gamma) \quad (5.15)$$

when $n = 3$ and $\gamma > 1$.

Summarizing the analysis above, we have:

Lemma 5.2. *Assume that $n = 2$ or $n = 3$, $\gamma > 1$, $\kappa = \bar{\kappa}(\gamma, \lambda)$, and $1 < \lambda < \lambda_n^\circ(\gamma)$. Then,*

$$V_4 < V_+. \quad (5.16)$$

Remark 5.1. *For later reference we record that, with $n = 2$ or $n = 3$, the function $\gamma \mapsto \lambda_n^\circ(\gamma)$ is continuous, strictly increasing, and bounded above by $\sqrt{n} < 2$. Also, the definitions of $\lambda_n^\circ(\gamma)$, $\hat{\lambda}_n(\gamma)$ and $\tilde{\lambda}_n(\gamma)$ give*

$$1 < \lambda_n^\circ(\gamma) \leq \hat{\lambda}_n(\gamma) \quad (5.17)$$

and

$$1 < \lambda_n^\circ(\gamma) \leq \tilde{\lambda}_n(\gamma) \quad (5.18)$$

for all $\gamma > 1$.

5.2. Presence and locations of P_4 - P_9 . The following lemma gives more precise information about the presence and location of the critical points P_4 - P_9 . We note that this is the first place where we exploit the freedom of choosing $\lambda > 1$ sufficiently close to 1; we will do so also in later results.

Lemma 5.3. *Assume that $n = 2$ or $n = 3$, $\gamma > 1$, $\kappa = \bar{\kappa}(\gamma, \lambda)$, and $1 < \lambda < \lambda_n^\circ(\gamma)$. Then,*

$$-1 < V_-, V_4 < V_+ < V_* < 0, \quad (5.19)$$

where V_\pm, V_4, V_* are given in (3.10), (3.6), (4.13), respectively. It follows that all of the critical points P_4 - P_9 are present with $P_6, P_8 \in L_+$ and $P_7, P_9 \in L_-$. Furthermore, we have that

$$V_- < V_4 \quad \text{and} \quad C_4 < 1 + V_4 \quad (5.20)$$

whenever $\lambda > 1$ is sufficiently close to 1 (depending on γ and n). In particular, for $\lambda \gtrsim 1$, P_4 (P_5) is located below (above) L_+ (L_-) in the upper (lower) half-plane.

Proof. We consider each of the inequalities in (5.19) in turn, from left to right.

- $-1 < V_-$: According to (3.10) this amounts to $\sqrt{\mathcal{Q}_n} < \mathbf{a}_n + 2$. We claim that $\mathbf{a}_n + 2 > 0$, i.e., $(\varepsilon - 2)\mu + m\varepsilon > 0$. This is immediate when $\varepsilon \geq 2$, while for $\varepsilon < 2$ it holds provided $\mu < \frac{m\varepsilon}{2-\varepsilon}$, which is an easy consequence of $\lambda < \hat{\lambda}_n(\gamma)$. According to (5.17) and the assumptions of the lemma, we therefore have $\mathbf{a}_n + 2 > 0$ for all cases under consideration. Thus, $\sqrt{\mathcal{Q}_n} < \mathbf{a}_n + 2$ holds if and only if $\mathcal{Q}_n < (\mathbf{a}_n + 2)^2$. Expanding the right-hand side, using the expressions from (3.11), and simplifying, yield the equivalent inequality $-(\varepsilon + 2)\mu < m\varepsilon$, which is trivially satisfied since $\varepsilon, \mu, m > 0$.
- $-1 < V_4$: According to (3.6) this amounts to $\lambda < 1 + \frac{n}{2}(\gamma - 1)$. Since $\tilde{\lambda}_n(\gamma) < 1 + \frac{n}{2}(\gamma - 1)$, this is an immediate consequence of (5.18) and the assumptions of the lemma.
- $V_- < V_+$: this is immediate from the definitions of V_\pm (cf. (3.10)).
- $V_4 < V_+$: This is the content of Lemma 5.2.
- $V_+ < V_*$: According to (3.10)-(3.11) and (4.13), this amounts to

$$mn\varepsilon\sqrt{\mathcal{Q}_n} < mn\varepsilon - (n(\varepsilon + 2) - 4)\mu. \quad (5.21)$$

As $n(\varepsilon + 2) - 4 > 0$ for all case under consideration, the right-hand side in (5.21) is positive provided $\mu < \frac{mn\varepsilon}{n(\varepsilon+2)-4}$. It is straightforward to verify that the latter is a consequence of $\lambda < \hat{\lambda}_n(\gamma)$, which holds according to (5.17) and the assumptions in the lemma. Squaring both sides of (5.21), and simplifying, we therefore get that (5.21) is equivalent to $(2 - n\varepsilon)\mu < n\varepsilon$. The latter inequality is trivially satisfied when $2 - n\varepsilon \leq 0$, while for $2 - n\varepsilon > 0$ it is equivalent to

$$\lambda < 1 + \frac{n(\gamma-1)}{2-n(\gamma-1)}.$$

Again, this is an easy consequence of $\lambda < \hat{\lambda}_n(\gamma)$.

- $V_* < 0$: This follows directly from (4.13) and the assumptions in the lemma.

Next, recall from (3.5) that P_4 - P_9 are present provided $g(V_4) > 0$ and $g(V_\pm) > 0$. The latter inequalities follow from the inequalities in (5.19) and the expression for $g(V)$ in (3.5). Also, as $V_+ > V_- > -1$, and P_6, P_8 (P_7, P_9) are located in the upper (lower) half-plane, it follows from (3.9) that $P_6, P_8 \in L_+$ ($P_7, P_9 \in L_-$).

Finally, consider the inequalities in (5.20), with $\gamma > 1$ and n fixed. From the expressions for V_- and V_4 in (3.10) and (3.6), we get that the inequality $V_- < V_4$ reduces to $-1 < -\frac{2}{2+n(\gamma-1)}$, which is trivially satisfied. Also, according to (3.5)-(3.6) and (5.19), the inequality $C_4 < 1 + V_4$ amounts to $V_4(\lambda + V_4) > n(V_4 - V_*)(1 + V_4)$. The limiting version at $\lambda = 1$ is the inequality $V_4(1 + V_4) > nV_4(1 + V_4)$ which is clearly satisfied for $V_4 = V_4|_{\lambda=1} = -\frac{2}{n\varepsilon+2} \in (-1, 0)$. It follows by continuity that both inequalities in (5.20) are satisfied whenever $\lambda > 1$ is sufficiently close to 1. \square

Remark 5.2. *A more detailed calculation reveals that for both $n = 2$ and $n = 3$, the inequality $V_- < V_4$ fails for pairs (γ, λ) with $\gamma \gtrsim 1$ and $\lambda \lesssim \hat{\lambda}_n(\gamma)$.*

We can now address the type of the critical points P_8 and P_9 .

5.3. Nodality of P_8, P_9 . According to (C3) it remains to determine the values of λ for which P_8 and P_9 are nodes. We start by recording some terminology and results from standard ODE theory (following the notation in [14]). The linearization of (2.14) at a critical point $P_c = (V_c, C_c)$ is

$$\frac{d\tilde{C}}{d\tilde{V}} = \frac{F_V\tilde{V} + F_C\tilde{C}}{G_V\tilde{V} + G_C\tilde{C}} \quad (5.22)$$

where $\tilde{V} = V - V_c$, $\tilde{C} = C - C_c$, and the partials F_V, F_C, G_V, G_C are evaluated at P_c . The Wronskian W and discriminant R^2 for the ODE (2.14) at P_c are defined by

$$W := F_C G_V - F_V G_C \quad (5.23)$$

and

$$R^2 := (F_C - G_V)^2 + 4F_V G_C \equiv (F_C + G_V)^2 - 4W. \quad (5.24)$$

In what follows, we write R for the positive square root of R^2 whenever the latter is positive. Assuming at present that $R^2 > 0$, we define the quantities

$$L_{1,2} = \frac{1}{2G_C}(F_C - G_V \pm R) \quad (5.25)$$

and

$$E_{1,2} = \frac{1}{2G_C}(F_C + G_V \pm R), \quad (5.26)$$

with signs chosen so that

$$|E_1| < |E_2|. \quad (5.27)$$

Note that the signs \pm in (5.25) and in (5.26) agree. We then have that integrals of (5.22) near P_c approach one of the curves

$$(\tilde{C} - L_1\tilde{V})^{E_1} = \text{constant} \times (\tilde{C} - L_2\tilde{V})^{E_2}. \quad (5.28)$$

Here, L_1 and L_2 are the *primary* and *secondary* slopes (or directions), respectively, at P_c . We observe that

$$W \equiv E_1 E_2 G_C^2. \quad (5.29)$$

Thus, under the assumption that $R^2 > 0$, the critical point P_c is a node (i.e., $\text{sgn } E_1 = \text{sgn } E_2$) when $W > 0$, and it is a saddle (i.e., $\text{sgn } E_1 = -\text{sgn } E_2$) when $W < 0$.

In the nodal case it follows from (5.28) that all but two of the integrals of (2.14) near P_c approach P_c with slope L_1 . The exceptions are the two integrals approaching P_c with slope L_2 (one from each side of the line $C - C_c = L_1(V - V_c)$). Similarly, in the saddle case, exactly four integrals of (2.14) near P_c approach P_c , two of them with slope L_1 and two with slope L_2 .

To guarantee that P_8 and P_9 are nodes, we require $R^2 > 0$ and $W > 0$ at P_8 and P_9 . Note that, according to (2.22), $W_8 \equiv W_9$ and $R_8^2 \equiv R_9^2$. It therefore suffices to consider one of these points, and we use P_9 . We begin with the sign of W_9 ; the more intricate condition $R^2 > 0$ is analyzed in Section 5.3.2.

5.3.1. *The Wronskian $W_9(n, \gamma, \lambda)$.* An elegant argument of Lazarus (see p. 323 in [14]) shows that the Wronskian W_9 factors as follows,

$$W_9 = W_9(n, \gamma, \lambda) = KC_9^2(V_9 - V_4)(V_9 - V_7), \quad (5.30)$$

where the positive constant K is given by

$$K = m(n\varepsilon + 2). \quad (5.31)$$

Recalling from Section 3.2 that $V_9 = V_+ > V_- = V_7$, we get from (5.30) that $W_9 > 0$ if and only if $V_+ > V_4$, which holds under the assumptions in Lemma 5.3. We therefore have:

Lemma 5.4. *Assume that $n = 2$ or $n = 3$, $\gamma > 1$, $\kappa = \bar{\kappa}(\gamma, \lambda)$, and $1 < \lambda < \lambda_n^\circ(\gamma)$. Assume in addition that the discriminant $R_9^2(n, \gamma, \lambda)$ is strictly positive. Then the Wronskian at P_9 satisfies $W_9(n, \gamma, \lambda) > 0$.*

5.3.2. *The discriminant $R_9^2(n, \gamma, \lambda)$.* As above we assume $n = 2$ or $n = 3$, $\gamma > 1$, $\kappa = \bar{\kappa}(\gamma, \lambda)$, and $1 < \lambda < \lambda_n^\circ(\gamma)$, and the goal is to provide sufficient conditions on λ to have $R_9^2 > 0$.

To simplify the notation we drop the subscript ‘9’ in most cases, evaluation at $P_9 = (V_9, C_9)$ being understood. Since the functions $D(V, C)$, $F(V, C)$, $G(V, C)$ all vanish at P_9 , we have

$$C = -(1 + V) \quad (5.32)$$

$$C^2 = k_1(1 + V)^2 - k_2(1 + V) + k_3 \quad (5.33)$$

$$C^2 = \frac{V(1+V)(\lambda+V)}{n(V-V_*)}. \quad (5.34)$$

By using these we have the following expressions for the partials of F and G at P_9 :

$$F_C = 2C^2 \quad (5.35)$$

$$F_V = C[k_2 - 2k_1(1 + V)] \quad (5.36)$$

$$G_C = 2nC(V - V_*) \equiv -2V(\lambda + V) \quad (5.37)$$

$$G_V = nC^2 - [(1 + V)(\lambda + V) + V(\lambda + V) + V(1 + V)] \equiv C[2V + \lambda - n(1 + V_*)]. \quad (5.38)$$

Recalling that $R^2 = (F_C + G_V)^2 - 4W$, and the expression (5.30) for W , a direct calculation shows that $R_9^2 = R_9^2(n, \gamma, \lambda) > 0$ holds if and only if

$$\begin{aligned} & 2[(n\varepsilon^2 + 2m\varepsilon - 4)\mu - m\varepsilon(n\varepsilon - 2)]\sqrt{q_n(\gamma, \lambda)} \\ & < [-2n\varepsilon^3 + (9n - 5)\varepsilon^2 - 4(n - 3)\varepsilon + 4(n - 5)]\mu^2 \\ & \quad + 2m\varepsilon(\varepsilon + 2)(2n\varepsilon - n + 3)\mu - m\varepsilon^2[2mn\varepsilon - (n^2 - 2n + 5)]. \end{aligned}$$

Thus,

- for $n = 2$, $R_9^2 > 0$ if and only if

$$\begin{aligned} 4(\gamma - 2)[(\gamma + 1)\mu - (\gamma - 1)]\sqrt{q_2(\gamma, \lambda)} & < (-4\gamma^3 + 25\gamma^2 - 34\gamma + 1)\mu^2 \\ & \quad + 2(\gamma^2 - 1)(4\gamma - 3)\mu - (4\gamma - 9)(\gamma - 1)^2, \end{aligned} \quad (5.39)$$

where

$$q_2(\gamma, \lambda) = (\gamma - 3)^2\mu^2 - 2(\gamma^2 - 1)\mu + (\gamma - 1)^2;$$

and,

- for $n = 3$, $R_9^2 > 0$ if and only if

$$(3\gamma - 5)[(\gamma + 1)\mu - 2(\gamma - 1)]\sqrt{\mathfrak{q}_3(\gamma, \lambda)} < -(3\gamma - 5)(\gamma^2 - 5\gamma + 2)\mu^2 \\ + 12(\gamma - 1)^2(\gamma + 1)\mu - 4(3\gamma - 5)(\gamma - 1)^2, \quad (5.40)$$

where

$$\mathfrak{q}_3(\gamma, \lambda) = (\gamma - 3)^2\mu^2 - 4(\gamma^2 - 1)\mu + 4(\gamma - 1)^2.$$

While numerical plots indicate that (5.39) ((5.40), respectively) holds whenever $\gamma > 1$ and $1 < \lambda < \lambda_2^\circ(\gamma)$ ($1 < \lambda < \lambda_3^\circ(\gamma)$, respectively), we have not been able to prove this. However, the following weaker assertion will suffice for our needs.

Lemma 5.5. *Assume that $n = 2$ or $n = 3$, $\gamma > 1$, $\kappa = \bar{\kappa}(\gamma, \lambda)$, and $1 < \lambda < \lambda_n^\circ(\gamma)$. Then $R_9^2(n, \gamma, \lambda) > 0$ whenever $\lambda > 1$ is sufficiently close to 1 (depending on γ and n).*

Proof. For $n = 2$, this follows directly by observing that along $\lambda \equiv 1$, (5.39) reduces to $-4(\gamma - 2)(\gamma - 1)^2 < -(4\gamma - 9)(\gamma - 1)^2$, which is trivially satisfied for all $\gamma > 1$, and the claim follows by continuity.

On the other hand, when $n = 3$, the two sides of (5.40) agree along $\lambda \equiv 1$. Letting $\mathfrak{l}(\gamma, \lambda)$ and $\mathfrak{r}(\gamma, \lambda)$ denote the left-hand and right-hand sides in (5.40), respectively, it thus suffices to verify the strict inequality

$$\frac{\partial \mathfrak{l}}{\partial \lambda} \Big|_{\lambda=1} < \frac{\partial \mathfrak{r}}{\partial \lambda} \Big|_{\lambda=1}.$$

A calculation shows that the latter inequality amounts to $4(3\gamma - 5)(\gamma^2 - 1) < 12(\gamma - 1)(\gamma^2 - 1)$, which is trivially satisfied for all $\gamma > 1$, and again the claim follows by continuity. \square

Definition 5.1. *For $n = 2$ or $n = 3$, $\gamma > 1$, and $\kappa = \bar{\kappa}(\gamma, \lambda)$, the pair (γ, λ) is called relevant provided $1 < \lambda < \lambda_n^\circ(\gamma)$, and $R_9^2(n, \gamma, \lambda) > 0$.*

Note that, according to Lemma 5.4, $W_9(n, \gamma, \lambda) > 0$ whenever (γ, λ) is relevant. By combining Lemma 5.5 and Lemma 5.4 with Proposition 4.2, we obtain:

Proposition 5.6. *Assume $n = 2$ or $n = 3$, $\gamma > 1$, and $\kappa = \bar{\kappa}(\gamma, \lambda)$. Then the pair (γ, λ) is relevant whenever $\lambda > 1$ is sufficiently close to 1, and in this case the constraints (C1), (C2), (C3) are all satisfied. In particular, P_8 and P_9 are nodes, and $P_{\pm\infty}$ are saddles.*

6. FURTHER PROPERTIES OF CRITICAL POINTS

To construct continuous similarity flows we need to determine the primary and secondary slopes at P_8 and P_9 under the assumptions of Proposition 5.6. We shall also need to compare these with the slopes of the zero-levels $\mathcal{F} = \{F = 0\}$ and $\mathcal{G} = \{G = 0\}$ at P_8 and P_9 . In addition, it will be useful to determine the types of the two critical points P_4 and P_5 (located off the critical lines L_\pm). Recalling the symmetries in (2.22), in particular the invariance of W and R^2 under $(V, C) \mapsto (V, -C)$, it suffices to analyze the critical points in the lower half-plane.

Throughout this section it is assumed in all calculations and statements that (γ, λ) is relevant according to Definition 5.1; in particular, $R_9^2 > 0$ and $W_9 > 0$.

6.1. Primary and secondary slopes at P_9 . In the following analysis we suppress the subscript ‘9’ in most cases, evaluation at P_9 being understood.

Lemma 6.1. *The primary and secondary slopes at P_9 are*

$$L_1 = \frac{1}{2G_C}(F_C - G_V - R) \quad \text{and} \quad L_2 = \frac{1}{2G_C}(F_C - G_V + R), \quad (6.1)$$

respectively.

Proof. The primary and secondary slopes are given by (5.25) and (5.26). Recall that the signs \pm in these equations agree. We claim that

$$F_C + G_V > 0. \quad (6.2)$$

Assuming this, it follows from (5.24), $W > 0$, and (5.27), that E_1 is given by choosing the ‘-’ sign in (5.26), and (6.1) follows.

It only remains to argue for (6.2). Using the expressions in (5.35), (5.38), together with (5.32), we have

$$F_C + G_V = 2C^2 + C[2V + \lambda - n(1 + V_*)] = C[\lambda - 2 - n(1 + V_*)]. \quad (6.3)$$

Since (γ, λ) is assumed relevant, (4.2) gives $1 + V_* > 0$, while the first part of Remark 5.1 gives $\lambda < 2$. As $C = C_9 < 0$, (6.3) therefore gives $F_C + G_V > 0$. \square

The next result provides the relative positions near P_9 of the level sets \mathcal{F} , \mathcal{G} (whose slopes are $-\frac{F_V}{F_C}$ and $-\frac{G_V}{G_C}$, respectively) and the straight lines through P_9 with slopes $L_{1,2}$.

Lemma 6.2. *At P_9 we have*

$$-\frac{G_V}{G_C} < L_1 < -\frac{F_V}{F_C} < -1 < 0 < L_2. \quad (6.4)$$

Proof. We first observe that (5.37)₁, Lemma 5.3, and $C < 0$ give

$$G_C = 2nC(V - V_*) > 0. \quad (6.5)$$

Using the expression for L_1 in (6.1) we therefore get that the leftmost inequality in (6.4) holds if and only if $F_C + G_V > R$. We showed in the proof of Lemma 6.1 that $F_C + G_V > 0$, and we have $R > 0$ by assumption. The inequality $F_C + G_V > R$ is therefore a direct consequence of (5.24)₂ and $W > 0$.

Next consider the inequality $-\frac{F_V}{F_C} < -1$, which, according to (5.35), is equivalent to $F_V > F_C$. Substituting the expressions in (5.35)-(5.36), and using (5.32), we obtain the equivalent inequality $k_2 < 2(k_1 - 1)(1 + V)$. Using the expressions for k_1, k_2 in (2.12), together with the expression for $V_9 = V_+$ given by (3.10)-(3.11), the last inequality reduces to $m(\gamma - 1)\sqrt{\Omega_n} > 0$, which trivially holds.

Next, using that $F_C > 0$, $G_C > 0$ (by (5.35) and (6.5)) and (6.1)₁, we have that $L_1 < -\frac{F_V}{F_C}$ holds if and only if

$$F_C(F_C - G_V) + 2F_V G_C < F_C R. \quad (6.6)$$

This inequality is trivially satisfied if the left-hand side is non-positive. If not we square both sides of (6.6) and use the first expression for R^2 in (5.24) to simplify, and obtain the equivalent inequality

$$F_V G_C (F_C G_V - F_V G_C) \equiv F_V G_C W > 0. \quad (6.7)$$

We just established $F_V > F_C > 0$ and $G_C > 0$ above, while $W > 0$ by assumption. Thus, (6.7) holds, and this verifies $L_1 < -\frac{F_V}{F_C}$ for all cases under consideration.

Finally, according to (6.1)₂ and (6.5), the inequality $L_2 > 0$ reduces to $F_C - G_V + R > 0$ which, by (5.24)₁, amounts to

$$F_C - G_V + \sqrt{(F_C - G_V)^2 + 4F_V G_C} > 0.$$

As $F_V > 0$, $G_C > 0$, this last inequality holds, establishing the rightmost inequality in (6.4). \square

The situation in the lower half-plane is given schematically in Figure 1. Observe that Figure 1 does not include certain parts of the zero-levels $\{F = 0\}$ and $\{G = 0\}$ (roughly those to the left of P_5 ; these are not relevant for what follows). Also, while Lemma 6.2 shows that the behavior near P_9 is accurately depicted, we omit the details for verifying that Figure 1 provides the correct global situation to the right of P_5 . (This requires a straightforward analysis of the polynomial functions F and G .) However, we record two properties that are useful for determining the flow

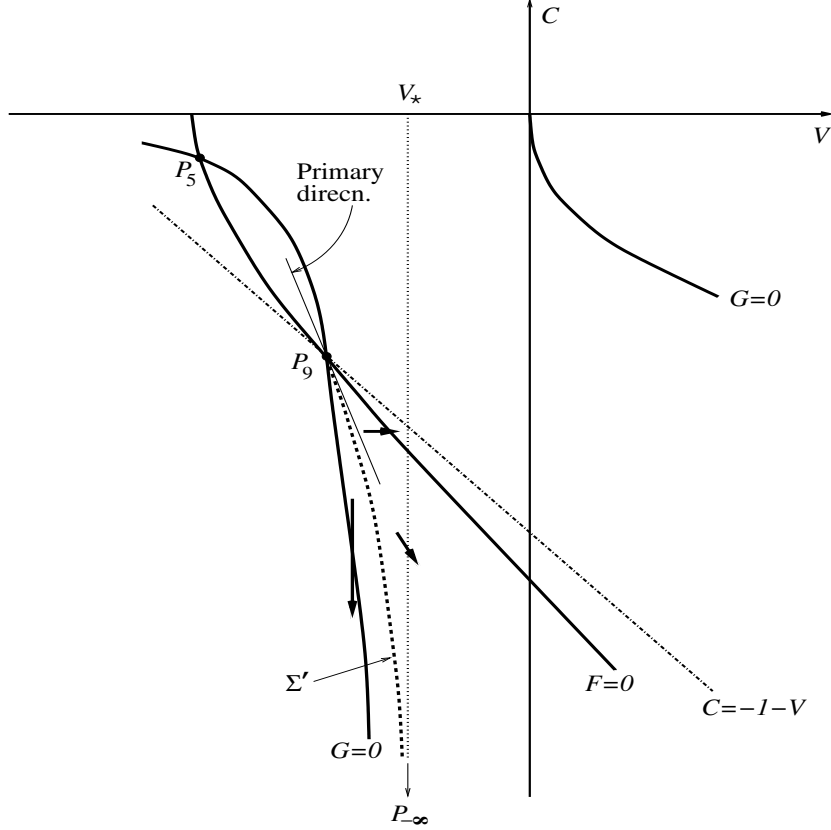


FIGURE 1. Schematic picture of the relative locations of the zero-level sets of F and G (solid thick curves), the primary direction (solid thin line), and the critical line $L_- = \{C = -1 - V\}$ (dash-dot) near P_9 . Also shown is the vertical asymptote $V = V_*$ of the zero-level of G (thin dotted), as well as the unique P_9P_∞ -trajectory Σ' (thick dotted). The three thick arrows indicate the direction of flow for solutions to the original ODE system (2.5)-(2.6) as $x > 0$ increases.

direction of the original similarity ODEs (2.5)-(2.6): (p1): Both $\{F = 0\}$ and $\{G = 0\}$ tend to infinity with asymptotically constant slopes in the 4th quadrant, with $\{G = 0\}$ everywhere located above $\{F = 0\}$; and (p2): With $C < 0$ fixed and $V \rightarrow +\infty$, it follows from (2.9), (2.8) that $G(V, C) < 0 < F(V, C)$.

6.2. The node-saddle connection P_9P_∞ . Referring again to Figure 1, let Ω be the unbounded open region in the 3rd quadrant of the (V, C) -plane which is bounded by the curves $\{V = V_*\}$, $\{G = 0\}$, and $\{F = 0\}$, i.e.,

$$\Omega = \{(V, C) \mid V < V_*, C < C_9, G(V, C) > 0, F(V, C) < 0\}.$$

It is then routine to use two properties (p1)-(p2) above to verify that trajectories inside Ω of the original similarity ODEs (2.5)-(2.6), move in a south-east manner as x increases. (Recall that $x > 0$ along such solutions, cf. the analysis in Section 3.1.) Furthermore, Ω contains no critical points and, as indicated by thick arrows in Figure 1, any trajectory that meets $\partial\Omega \setminus \{P_9\}$ must exit Ω . Finally, according to Proposition 5.6, P_∞ is a saddle point and P_9 is a node. It follows by continuity that among the infinitely many trajectories entering Ω at P_9 , there is a unique trajectory, denoted Γ' , which connects P_9 to P_∞ .

6.3. The critical points P_4 and P_5 . The locations of the critical points P_4 and P_5 are given by Lemma 5.3. To determine their types, we make use of the following expressions for the Wronskian at P_4 and P_5 (cf. (5.30); for proofs see p. 323 in [14]):

$$W_4 = W_5 = W_5(n, \gamma, \lambda) = KC_5^2(V_5 - V_7)(V_5 - V_9), \quad (6.8)$$

where the positive constant K is given in (5.31). Recall that $V_5 = V_4$, $V_7 = V_-$, and $V_9 = V_+$. Therefore, by combining Lemma 5.3 and Lemma 5.5, we obtain that $W_4 = W_5 < 0$, so that P_4 and P_5 are saddle points whenever (γ, λ) is relevant.

Summarizing the analysis in Sections 5 and 6, we have:

Proposition 6.3. *Assume $n = 2$ or $n = 3$, $\gamma > 1$, $\kappa = \bar{\kappa}(\gamma, \lambda)$, and $\lambda > 1$ is sufficiently close to 1. Then:*

- All of the critical points P_4 - P_9 are present;
- P_8 and P_9 are nodes for (2.14);
- P_7 and P_9 are located along L_- within the half-strip $\{(V, C) \mid -1 < V < V_*, C < 0\}$;
- P_6 and P_8 are located along L_+ within the half-strip $\{(V, C) \mid -1 < V < V_*, C > 0\}$;
- P_4 and P_5 are saddles for (2.14);
- P_5 is located within the set $\{(V, C) \mid V_- < V < V_+, -(1+V) < C < 0\}$;
- P_4 is located within the set $\{(V, C) \mid V_- < V < V_+, 0 < C < 1+V\}$;
- There is a unique trajectory Γ' of the original similarity ODEs (2.5)-(2.6) which joins P_9 to $P_{-\infty}$.

7. BLOWUP SOLUTIONS CONTINUOUS AWAY FROM THE POINT OF COLLAPSE

We proceed to argue for the statements in Theorem 1.1. The main issue is to establish that, for $n = 3$, $\gamma > 1$, $\kappa = \bar{\kappa}(\gamma, \lambda)$, and with $\lambda > 1$ sufficiently close to 1, the particular trajectory of (2.5)-(2.6) which passes *vertically* through the origin P_1 in the (V, C) -plane, connects the nodes P_8 and P_9 . Thanks to the symmetries in (2.22), it suffices to show that its part in the lower half-plane, denoted Σ , connects P_1 to P_9 .

To argue for this, we shall show in Section 7.1 below that, under the stated conditions on n , γ , κ , and λ , the trajectory Σ is located *strictly* between two parabolae (or, rather, parts of parabolae)

$$\Pi_1 = \{V = -\beta_1 C^2, C_5 < C < 0\}, \quad \Pi_2 = \{V = -\beta_2 C^2, C_9 < C < 0\},$$

in the third quadrant and which satisfy

$$\beta_1 > \beta_2, \quad P_5 \in \Pi_1, \quad \text{and} \quad P_9 \in \Pi_2. \quad (7.1)$$

Let \mathcal{R} denote the region in the 3rd quadrant which is bounded by Π_1 , Π_2 , and that part of $\{G = 0\}$ which is located between P_5 and P_9 ; see Figure 2. It follows from the expressions for F , G , and D that trajectories of (2.5)-(2.6) move in a south-west manner within \mathcal{R} as $x > 0$ increases.

The argument in Section 7.1 will establish the following properties:

- (A) Σ starts out from P_1 strictly between Π_1 and Π_2 ;
- (B) Any trajectory of (2.5)-(2.6) which meets Π_1 moves into \mathcal{R} ; and
- (C) Any trajectory of (2.5)-(2.6) which meets Π_2 moves into \mathcal{R} .

Taking these properties for granted for now, it follows that Σ does not exit \mathcal{R} along Π_1 or Π_2 . It therefore reaches $\{G = 0\}$ (vertically) at a point located *strictly* between P_5 and P_9 , and enters the “eye-shaped” region

$$\mathcal{E} := \{(V, C) \mid V_5 < V < V_9, G(V, C) < 0 < F(V, C)\}. \quad (7.2)$$

Recalling that $x > 0$ along solutions of the similarity ODEs (2.5)-(2.6) in the lower half-plane, it is routine to verify that \mathcal{E} is a trapping region for the system (2.5)-(2.6). Any solution of (2.5)-(2.6)

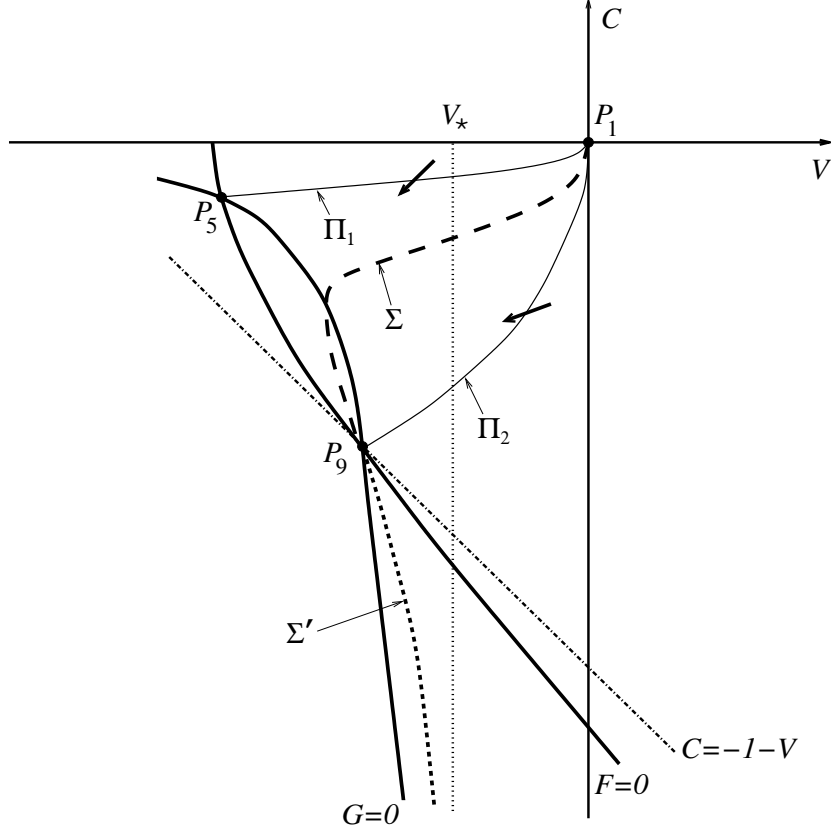


FIGURE 2. Schematic picture showing the Σ trajectory (thick long dashes) which leaves the origin P_1 vertically and connects P_1 to P_9 . Σ is bounded above and below by the parabolic barriers Π_1 and Π_2 (thin curves), respectively, before entering the eye-shaped region between P_5 and P_9 . The two thick arrows indicate how solutions to the original ODE system (2.5)-(2.6) cross the barriers as $x > 0$ increases.

which enters \mathcal{E} must therefore approach the node at P_9 as x increases. Thus, modulo the properties (A), (B), (C), we have that Σ connects P_1 to P_9 .

Having reached P_9 , the trajectory Σ is continued as the unique node-saddle trajectory Γ' connecting P_9 to $P_{-\infty}$ (cf. Section 6.2); see Figure 2.

Next, let Σ_{\circ} and Σ'_{\circ} denote the reflections of Σ and Σ' , respectively, about the V -axis. With these we define the trajectory

$$\Gamma := \Sigma'_{\circ} \cup \Sigma_{\circ} \cup \Sigma \cup \Sigma'. \quad (7.3)$$

Recall from Section 3.4 that approaching $P_{+\infty}$ along Σ'_{\circ} corresponds to $x \rightarrow -\infty$, and that approaching $P_{-\infty}$ along Σ' corresponds to $x \rightarrow +\infty$. It follows that Γ provides a trajectory connecting $P_{+\infty}$ to $P_{-\infty}$ via P_8 , P_1 , and P_9 , and that the corresponding solution $(V(x), C(x))$ of the similarity ODEs (2.5)-(2.6) is defined and *continuous* for all $x \in (-\infty, \infty)$. With Γ so constructed we obtain the velocity and sound speed of the corresponding Euler flow from (1.10)_{3,4}.

Remark 7.1. *We note that, strictly speaking, we have the freedom of choosing any positive $x_9 > 0$, say, and then fixing the solution $(V(x), C(x))$ that traverses Γ by insisting that $(V(x_9), C(x_9)) = P_9$. Choosing different values for x_9 will give physically distinct Euler flows; however, these are all trivially related via space-time scalings.*

To complete the construction of the sought-for solution we need to specify the density field. For this we choose any positive constant for the right-hand side of (2.21), fixing the function $R(x)$ along the solution under consideration, and define the associated flow variables $(\rho(t, r), u(t, r), c(t, r))$ according to (1.10). This will complete the construction of a globally defined, radial Euler flow which, by construction is continuous everywhere except at $(t, r) = (0, 0)$, where it suffers amplitude blowup (in ρ, u, c, p , and θ). Modulo the properties (A), (B), (C), this establishes parts (i), (ii), and (iii) of Theorem 1.1. The next section provides the details of proving (A), (B), (C), and part (iv) of Theorem 1.1 is established in Section 7.2.

7.1. Analysis of the Σ trajectory. To carry out the analysis outlined above, we first calculate the leading (quadratic) order behavior of Σ near the origin P_1 . That is, we determine $\beta > 0$ such that

$$\Sigma = \{V = -\beta C^2 + O(C^3) \text{ for } C \lesssim 0\}.$$

Until further notice it is assumed that $n = 2$ or $n = 3$, $\gamma > 1$, $\kappa = \bar{\kappa}$, and $\lambda > 1$. We consider V as a function of C along Σ and use (2.14), in the form $\frac{dV}{dC} = \frac{G(V, C)}{F(V, C)}$, to calculate

$$\frac{d^2V}{d^2C} = \frac{G(FG_V - GF_V) + F(FG_C - GF_C)}{F^3}. \quad (7.4)$$

From (2.8)-(2.9), and with $V \approx -\beta C^2$, we have to leading order along Σ near P_1 that

$$\begin{aligned} G &= nC^2(V - V_*) - V(1 + V)(\lambda + V) \approx (\beta\lambda - nV_*)C^2 \\ G_V &= nC^2 - (1 + V)(\lambda + V) - V(\lambda + V) - V(1 + V) \approx -\lambda \\ G_C &= 2nC(V - V_*) \approx -2nV_*C \\ F &= C[C^2 - k_1(1 + V)^2 + k_2(1 + V) - k_3] \approx -\lambda C \\ F_V &= C[k_2 - 2k_1(1 + V)] \approx (k_2 - 2k_1)C \\ F_C &= 3C^2 - k_1(1 + V)^2 + k_2(1 + V) - k_3 \approx -\lambda, \end{aligned}$$

where we have used (2.13) and the fact that $\alpha = 0$ since $\kappa = \bar{\kappa}$; also, V_* is given by (4.13). Using these expressions in (7.4) gives

$$-2\beta = \left. \frac{d^2V}{d^2C} \right|_{C=0} = \frac{2nV_*}{\lambda},$$

or

$$\beta = -\frac{nV_*}{\lambda} = \frac{2\mu}{\varepsilon\lambda}. \quad (7.5)$$

Next, the parabola

$$\Pi_1 = \{V = -\beta_1 C^2, C_5 < C < 0\}$$

is defined by the requirement that it passes through P_5 , giving

$$\beta_1 = -\frac{V_5}{C_5^2} = \frac{n(V_* - V_5)}{(1 + V_5)(\lambda + V_5)} = \frac{2(2 + n\varepsilon)}{n\lambda\varepsilon^2}, \quad (7.6)$$

where we have used (3.5) and (3.6) (recall that $V_5 = V_4$). Similarly, the parabola

$$\Pi_2 = \{V = -\beta_2 C^2, C_9 < C < 0\}$$

is defined by the requirement that it passes through P_9 , giving

$$\beta_2 = -\frac{V_9}{C_9^2} = -\frac{V_+}{(1 + V_+)^2}, \quad (7.7)$$

where we have used that $P_9 \in L_-$, and where $V_9 = V_+$ is given by (3.10)-(3.11). Note that it follows from Proposition 6.3 that P_5 is located north-west of P_9 within the triangle

$$\mathcal{T} := \{(V, C) \mid -1 < -1 - V < C < 0\}. \quad (7.8)$$

in the third quadrant (cf. Figure 2).

As argued above, in order to show that Σ meets $\{G = 0\}$ between P_5 and P_9 , it suffices to establish properties (A), (B), (C), which amount to the following:

(A) Σ starts out from P_1 between Π_1 and Π_2 , i.e.,

$$\beta_1 > \beta > \beta_2; \quad (7.9)$$

(B) Whenever a trajectory $(V(C), C)$ of (2.14) crosses Π_1 at a point $(-\beta_1 C^2, C)$, with $C_5 < C < 0$, we have

$$\frac{dV}{dC} \Big|_{\Pi_1} = \frac{G(-\beta_1 C^2, C)}{F(-\beta_1 C^2, C)} < -2\beta_1 C; \quad (7.10)$$

this guarantees that solutions to (2.5)-(2.6) cross Π_1 into the region \mathcal{R} as x increases;

(C) Whenever a trajectory $(V(C), C)$ of (2.14) crosses Π_2 at a point $(-\beta_2 C^2, C)$, with $C_9 < C < 0$, we have

$$\frac{dV}{dC} \Big|_{\Pi_2} = \frac{G(-\beta_2 C^2, C)}{F(-\beta_2 C^2, C)} > -2\beta_2 C; \quad (7.11)$$

this guarantees that solutions to (2.5)-(2.6) cross Π_2 into the region \mathcal{R} as x increases.

We proceed to verify that (A), (B), and (C) are all satisfied for $n = 3$, $\gamma > 1$, $\kappa = \bar{\kappa}$, provided $\lambda > 1$ is sufficiently close to 1 (depending on γ). We note that it is only in verifying property (A) that we need to restrict to $n = 3$.

7.1.1. Property (A). Substituting from (7.5) and (7.6), and rearranging, we have that $\beta_1 > \beta$ amounts to $2 + n\varepsilon > \mu n\varepsilon$, which is trivially satisfied whenever $\mu = \lambda - 1 \gtrsim 0$.

The analysis of the second inequality $\beta > \beta_2$ is more involved, and, as we shall see, its validity requires $n = 3$. Considering V_* and V_+ as functions of μ , we have

$$V_* = -\frac{2\mu}{n\varepsilon} \quad \text{and} \quad V_+ = -\frac{2\mu}{n\varepsilon} + O(\mu^2), \quad (7.12)$$

where we have used (4.13) and (3.10)-(3.11). Using these to Taylor expand β_2 in (7.7) gives

$$\beta_2 = \frac{2}{m\varepsilon}\mu + \frac{2(\varepsilon+4)}{m^2\varepsilon^2}\mu^2 + O(\mu^3). \quad (7.13)$$

Also, according to (7.5), we have

$$\beta = \frac{2}{\varepsilon}\mu - \frac{2}{\varepsilon}\mu^2 + O(\mu^3),$$

It follows from these expressions that the inequality $\beta > \beta_2$ fails for $n = 2$ ($m = 1$), while it is satisfied for $n = 3$ ($m = 2$), when $\mu \gtrsim 0$ (depending on ε , i.e., on γ). Consequently, in what follows we restrict attention to $n = 3$.

7.1.2. Property (B). With $n = 3$, $\varepsilon = \gamma - 1 > 0$, and $\kappa = \bar{\kappa}$ we have

$$\beta_1 = \frac{2(3\varepsilon+2)}{3\lambda\varepsilon^2}, \quad V_* = -\frac{2\mu}{3\varepsilon}, \quad V_5 = V_4 = -\frac{2\lambda}{3\varepsilon+2}, \quad C_5^2 = \frac{3\lambda^2\varepsilon^2}{(3\varepsilon+2)^2} \quad (7.14)$$

where we have used (7.6), (4.13), (3.6), and (3.5). Also, from (2.12), we have

$$k_1 = \varepsilon + 1, \quad k_2 = \frac{(2+\mu)\varepsilon-2\mu}{2}, \quad \text{and} \quad k_3 = \frac{\mu\varepsilon}{2}. \quad (7.15)$$

As $F > 0$ along Π_1 , we have that (7.10) holds if and only if

$$G(-\beta_1 C^2, C) < -2\beta_1 C F(-\beta_1 C^2, C) \quad \text{for } C_5 < C < 0. \quad (7.16)$$

Using the expressions for F and G from (2.8)-(2.9), together with (7.14)-(7.15), rearranging and dividing through by $\beta_1 C^2 > 0$, and finally setting $Z = C^2$, we obtain the equivalent inequality

$$(2\varepsilon + 1)\beta_1^2 Z^2 + \{1 + [(\mu - 2)\varepsilon - (\mu + 2)]\beta_1\} Z + (\lambda - \frac{2\mu}{\beta_1\varepsilon}) < 0 \quad \text{for } 0 < Z < Z_5 := C_5^2. \quad (7.17)$$

We proceed to argue that (7.17) is satisfied whenever $\lambda \gtrsim 1$ (i.e., $\mu \gtrsim 0$). Denoting the left-hand side of (7.17) by $\phi(Z)$, we have

$$\phi'(Z) = 2(2\varepsilon + 1)\beta_1^2 Z + 1 + [(\mu - 2)\varepsilon - (\mu + 2)]\beta_1.$$

Direct evaluations, using (7.14), then give

- $\phi(Z_5) = 0$ for any $\lambda > 1$ (note that this reflects the fact that (7.16), and hence (7.17), is satisfied with equality for $Z = Z_5$ since $F(P_5) = G(P_5) = 0$); and
- $\phi'(Z_5) = -\frac{9\varepsilon+4}{3\varepsilon} + O(\mu) < 0$ for $\lambda \gtrsim 1$.

As $\phi(Z)$ is a quadratic polynomial in Z with a positive leading coefficient, it follows that $\phi(Z) > 0$ for $0 < Z < Z_5$, establishing (7.17). This shows that Property (B) holds whenever $\lambda > 1$ is sufficiently close to 1 (depending on γ).

7.1.3. *Property (C)*. We assume $n = 3$, $\varepsilon = \gamma - 1 > 0$, and $\kappa = \bar{\kappa}$. As $F > 0$ along Π_2 , we have that (7.11) holds if and only if

$$-2\beta_2 C F(-\beta_2 C^2, C) < G(-\beta_2 C^2, C) \quad \text{for } C_9 < C < 0. \quad (7.18)$$

Using the expressions for F and G from (2.8)-(2.9) together with (7.15), rearranging and dividing through by $\beta_2 C^2 > 0$, and finally setting $Z = C^2$, we obtain the equivalent inequality

$$(2\varepsilon + 1)\beta_2^2 Z^2 + \{1 + [(\mu - 2)\varepsilon - (\mu + 2)]\beta_2\} Z + (\lambda - \frac{2\mu}{\beta_2\varepsilon}) < 0, \quad \text{for } 0 < Z < Z_9 := C_9^2. \quad (7.19)$$

We proceed to argue that (7.19) is satisfied whenever $\lambda \gtrsim 1$. Denoting the left-hand side of (7.19) by $\psi(Z)$, direct evaluations, using (7.13) give

- $\psi(0) = -1 + O(\mu) < 0$ for $\lambda \gtrsim 1$;
- $\psi(Z_9) = 0$ for any $\lambda > 1$ (note that this reflects the fact that (7.18), and hence (7.19), is satisfied with equality for $Z = Z_9$ since $F(P_9) = G(P_9) = 0$).

As $\psi(Z)$ is a quadratic polynomial in Z with a positive leading coefficient, it follows that $\psi(Z) < 0$ for $0 < Z < Z_9$, establishing (7.19). This shows that Property (C) holds whenever $\lambda > 1$ is sufficiently close to 1 (depending on γ).

With this we have argued for parts (i), (ii), and (iii) of Theorem 1.1.

7.2. **Proof of part (iv) of Theorem 1.1.** With the existence of the continuous solution trajectory Γ in (7.3) established, part (iv) of Theorem 1.1 is argued for as follows.

Recall from the construction above that the trajectory $\Sigma_{89} := \Sigma \cup \Sigma_\circ$ is the unique $P_8 P_9$ -connection that passes vertically through the origin P_1 . For the parameter regime described in Theorem 1.1, it was established above that Σ_{89} meets $\{G = 0\}$ at a point strictly between P_5 and P_9 in the lower half-plane. As Σ_\circ is the reflection of Σ about the V -axis, it follows that Σ_{89} also meets $\{G = 0\}$ at a symmetrically located point located strictly between P_4 and P_8 in the upper half-plane. It now follows by continuity that there are nearby trajectories connecting the node at P_8 to the node at P_9 via P_1 . Any such ‘‘perturbed’’ $P_8 P_9$ trajectory $\tilde{\Gamma}_{89}$ passes through P_1 with a (large) strictly positive or (large) strictly negative slope. We note that $\tilde{\Gamma}_{89}$ must arrive and leave P_1 with the same slope; see Section 8.2.1 below. With the same notation as in (7.3) we therefore have that

$$\tilde{\Gamma} := \Sigma'_\circ \cup \tilde{\Gamma}_{89} \cup \Sigma'. \quad (7.20)$$

is the trajectory of a solution $(\tilde{V}(x), \tilde{C}(x))$ to the similarity ODEs (2.5)-(2.6) which is defined and continuous for all $x \in (-\infty, \infty)$.

Finally, if $\tilde{\Gamma}_{89}$ passes through P_1 with a positive slope $\ell > 0$, then we are in Case 1 described in Section 3.1, and the fluid is everywhere flowing away from the center of motion at time $t = 0$. Similarly, if $\tilde{\Gamma}_{89}$ passes through P_1 with a negative slope $\ell < 0$, Case 2 in Section 3.1 applies, and the fluid is everywhere flowing toward the center of motion at time $t = 0$.

This concludes the proof of Theorem 1.1.

8. ADDITIONAL REMARKS

8.1. Blowup with a converging or diverging velocity field. As noted earlier, since $\lambda > 1$ and $\bar{\kappa} < 0$, all the solutions constructed above suffer blowup of density and pressure at the center of motion at time of collapse. Also, in Case 2 above the fluid is everywhere moving toward the origin $r = 0$ at time of collapse (cf. discussion in Section 3.1). It is surprising that, under these circumstances, no shock wave appears in the flows under consideration. We interpret this as demonstrating how compressibility, which is typically seen as a necessary ingredient in shock formation, can play a dual role in preventing shocks from developing.

Next, consider Case 1: Again the density blows up at $r = 0$ at time of collapse, but this now occurs while all fluid particles are moving away from the origin. It might seem that the latter property should tend to dilute the fluid, and thus prevent blowup of the density (recall that the density is bounded at any time strictly prior to collapse). However, what determines the rate of change of density along particle trajectories (i.e., $\dot{\rho} = \rho_t + u\rho_r = -\rho u_r$), is the sign of the velocity gradient u_r . For the self-similar flows under consideration

$$\dot{\rho} = -\frac{1}{\lambda} r^{\bar{\kappa}-\lambda} R(x) \left(\lambda V'(x) - \frac{V(x)}{x} \right).$$

In Case 1 we have $\frac{V(x)}{x} \rightarrow V'(0) < 0$ as $x \rightarrow 0$, so that

$$\dot{\rho}(0, r) = -\frac{1}{\lambda} r^{\bar{\kappa}-\lambda} R(0) (\lambda - 1) V'(0) > 0.$$

This shows that all fluid particles undergo an increase in density at time $t = 0$ in this case, and that this increase is more pronounced the closer the particle is to the center of motion.

8.2. On uniqueness. As indicated in Section 1, it is reasonable to ask if the strong singularities displayed by the type of solutions considered above could yield examples of non-unique continuation.

In this section we consider two possible scenarios for non-uniqueness. While one is easily dispelled with, the other requires more analysis to evaluate.

8.2.1. Passing through P_1 with a kink. Recall from Section 3.1 that the origin P_1 is a star point for the reduced similarity ODE (2.14), with trajectories approaching with any slope $\ell \in [-\infty, +\infty]$. Consider the trajectory Γ which was built in Section 7; its P_8P_9 -part (i.e., $\Sigma_\circ \cup \Sigma$) was constructed specifically to pass vertically through the origin P_1 . Having reached P_1 from P_8 along Σ_\circ , we could try to leave P_1 along a trajectory $\tilde{\Sigma}$ which is a slight perturbation of Σ - slight enough that $\tilde{\Sigma}$ still connects P_1 to P_9 . With notation as in (7.3), we would thus obtain a complete trajectory $\tilde{\Gamma} := \Sigma'_\circ \cup \Sigma_\circ \cup \tilde{\Sigma} \cup \Sigma'$, which connects $P_{+\infty}$ to $P_{-\infty}$, via P_8 and P_9 , and passes through P_1 . This would appear to generate an Euler flow which agrees for $t < 0$ with the one corresponding to the trajectory Γ , but it would differ from it for $t > 0$.

However, in contrast to Γ , the trajectory $\tilde{\Gamma}$ passes through P_1 with a kink, and this renders the corresponding Euler flow unphysical. Indeed, since $\tilde{\Gamma}$ approaches P_1 with different slopes as $x \rightarrow 0\pm$, (3.2) shows that at least one of $\frac{V(x)}{x}$ or $\frac{C(x)}{x}$ must suffer a jump as x passes through zero. According to (1.10) this gives an Euler flow which suffers an unphysical jump in velocity or in sound speed (and thus in density) at all locations $r > 0$ at time $t = 0$.

8.2.2. Non-uniqueness via an outgoing shock? The second scenario is more involved. For this we consider using a solution of the type described by Theorem 1.1 up to time of collapse, but then inserting an outgoing shock in the flow for $t > 0$ and emanating from $(t, r) = (0, 0)$.

For a solution as described by Theorem 1.1, consider the point $P(x) = (V(x), C(x))$ as it traverses the P_1P_9 -trajectory Σ for $0 \leq x \leq x_9$. For each such x -value we calculate the point $P_H(x) =$

$(V_H(x), C_H(x))$ with the property that the physical states corresponding to $P(x)$ and $P_H(x)$ satisfy the Rankine-Hugoniot relations for an admissible 3-shock. We refer to

$$\Sigma_H := \{(V_H(x), C_H(x)) \mid 0 < x < x_9\}$$

as the Hugoniot locus of Σ . (It follows from the Rankine-Hugoniot conditions and admissibility that Σ_H is a uniquely determined and differentiable curve located below the critical line L_- ; see [8, 14]. We omit the details.)

If the curve Σ_H intersects the $P_9P_{-\infty}$ -trajectory Σ' constructed earlier, for an x -value $x_s \in (0, x_9)$, then we would have an example of non-unique continuation for the Euler system. Specifically, one solution would be the earlier constructed flow described by Theorem 1.1 which moves along the trajectory Γ . The other solution would be constructed by using the part of Γ corresponding to $x < x_s$, then jumping to the point $P_H(x_s) \in \Sigma'$, and finally moving along Σ' as x increases from x_s to $+\infty$. The two corresponding Euler flows would agree up to time of collapse, but differ for $t > 0$ as one contains a shock and the other does not.

To determine whether the Hugoniot locus Σ_H can in fact intersect the trajectory Σ' turns out to be somewhat subtle. What we *can* say is the following. First, it follows from the Rankine-Hugoniot conditions that if \mathcal{C} is a differentiable curve (a trajectory of (2.14) or not) which tends to a point \bar{P} on the critical line L_- , then its Hugoniot locus approaches the same point. A further analysis shows that if \mathcal{C} approaches \bar{P} with slope σ , then its Hugoniot locus tends to \bar{P} with the slope

$$\sigma_H(\sigma) := \frac{\gamma-1}{2} + (\gamma+1) \frac{(\sigma - \frac{\gamma-1}{2})}{(\gamma-3-4\sigma)}. \quad (8.1)$$

(In particular, if \mathcal{C} is a trajectory of (2.14) which approaches L_- at a non-triple point, then (2.16) shows that it does so with slope $\sigma = \frac{\gamma-1}{2}$, and it follows from (8.1) that $\sigma_H = \sigma$ in this case.) Applying (8.1) to $\mathcal{C} = \Sigma$, which approaches the triple point $\bar{P} = P_9 \in L_-$ with the primary slope L_1 (cf. Lemma 6.1), we get that Σ_H approaches P_9 with slope $\sigma_H(L_1)$. According to Lemma 6.2 we have $L_1 < -1$ for the solutions under consideration, which, according to (8.1), gives $\sigma_H(L_1) > -1$. This implies that, at least near P_9 , the Hugoniot locus Σ_H is located within $\{V < V_9\}$, and thus does *not* meet Σ' , which is located within the strip $\{V_9 < V < V_*\}$.

This indicates that, in the isentropic setting under consideration, the flows described by Theorem 1.1 can *not* be “tweaked” to give examples of non-unique continuation for the compressible Euler system. However, we have not been able to settle this issue, e.g. by showing that the entire Hugoniot locus Σ_H is located within $\{V < V_9\}$ (as indicated by numerical tests). It would be of interest to provide a conclusive answer; the recent detailed analysis in [8] might be of help with this.

REFERENCES

- [1] K. V. Brushlinskii and Ya. M. Kazhdan, *On auto-models in the solution of certain problems of gas dynamics*, Russian Math. Surveys **18** (1963), 1–22.
- [2] Tristan Buckmaster, Gonzalo Cao-Labora, and Javier Gómez-Serrano, *Smooth self-similar imploding profiles to 3D compressible Euler*, Quart. Appl. Math. **81** (2023), no. 3, 517–532, DOI 10.1090/qam/1661. MR4623212
- [3] Jiajie Chen, Giorgio Cialdea, Steve Shkoller, and Vlad Vicol, *Vorticity blowup in 2D compressible Euler equations*, arXiv:2407.06455 (2024).
- [4] R. Courant and K. O. Friedrichs, *Supersonic flow and shock waves*, Springer-Verlag, New York, 1976. Reprinting of the 1948 original; Applied Mathematical Sciences, Vol. 21. MR0421279 (54 #9284)
- [5] G. Guderley, *Starke kugelige und zylindrische Verdichtungsstöße in der Nähe des Kugelmittelpunktes bzw. der Zylinderachse*, Luftfahrtforschung **19** (1942), 302–311 (German). MR0008522
- [6] Philip Hartman, *Ordinary differential equations*, Classics in Applied Mathematics, vol. 38, Society for Industrial and Applied Mathematics (SIAM), Philadelphia, PA, 2002. Corrected reprint of the second (1982) edition [Birkhäuser, Boston, MA; MR0658490 (83e:34002)]; With a foreword by Peter Bates. MR1929104
- [7] C. Hunter, *On the collapse of an empty cavity in water*, J. Fluid Mech. **8** (1960), 241–263.
- [8] Juhui Jang, Jiaqi Liu, and Matthew Schrecker, *Converging/diverging self-similar shock waves: from collapse to reflection*, SIAM J. Math. Analysis, to appear (2024).

- [9] Helge Kristian Jenssen and Alexander Johnson, *Gradient Blowup Without Shock Formation in Compressible Euler Flow*, *Physics of Fluids* **36** (2024), 026125, DOI 10.1063/5.0185592.
- [10] Helge Kristian Jenssen and Charis Tsikkou, *On similarity flows for the compressible Euler system*, *J. Math. Phys.* **59** (2018), no. 12, 121507, 25, DOI 10.1063/1.5049093. MR3894017
- [11] ———, *Multi-d isothermal Euler flow: existence of unbounded radial similarity solutions*, *Phys. D* **410** (2020), 132511, 14, DOI 10.1016/j.physd.2020.132511. MR4091348
- [12] ———, *Amplitude blowup in radial isentropic Euler flow*, *SIAM J. Appl. Math.* **80** (2020), no. 6, 2472–2495, DOI 10.1137/20M1340241. MR4181105
- [13] ———, *Radially symmetric non-isentropic Euler lows: Continuous blowup with positive pressure*, *Phys. Fluids* **35** (2023), 016117.
- [14] Roger B. Lazarus, *Self-similar solutions for converging shocks and collapsing cavities*, *SIAM J. Numer. Anal.* **18** (1981), no. 2, 316–371.
- [15] Frank Merle, Pierre Raphaël, Igor Rodnianski, and Jeremie Szeftel, *On the implosion of a compressible fluid I: Smooth self-similar inviscid profiles*, *Ann. of Math. (2)* **196** (2022), no. 2, 567–778, DOI 10.4007/annals.2022.196.2.3. MR4445442
- [16] ———, *On the implosion of a compressible fluid II: Singularity formation*, *Ann. of Math. (2)* **196** (2022), no. 2, 779–889, DOI 10.4007/annals.2022.196.2.4. MR4445443
- [17] B. L. Roždestvenskii and N. N. Janenko, *Systems of quasilinear equations and their applications to gas dynamics*, Russian edition, *Translations of Mathematical Monographs*, vol. 55, American Mathematical Society, Providence, RI, 1983. MR0694243
- [18] L. I. Sedov, *Similarity and dimensional methods in mechanics*, “Mir”, Moscow, 1982. Translated from the Russian by V. I. Kisin. MR693457
- [19] K. P. Stanyukovich, *Unsteady motion of continuous media*, Translation edited by Maurice Holt; literal translation by J. George Adashko, Pergamon Press, New York-London-Oxford-Paris, 1960. MR0114423

H. K. JENSSEN, DEPARTMENT OF MATHEMATICS, PENN STATE UNIVERSITY, UNIVERSITY PARK, STATE COLLEGE, PA 16802, USA (jenssen@math.psu.edu).